Report on volcanic plume measurements on volcanoes in Papua New Guinea

S. Arellano[a], B. Galle[a], K. Mulina[b], J. Wallius[c], B. McCormick[d], L. Salem[d], R. D'aleo[e], P. Barry[f], I. Itikarai[b]

[a]Department of Earth and Space Sciences, Chalmers University of Technology, Gothenburg, Sweden
[b]Rabaul Volcano Observatory, Rabaul, Papua New Guinea
[c]Department of Earth Sciences, Uppsala University, Uppsala, Sweden
[d]Department of Earth Sciences, University of Cambridge, Cambridge, United Kingdom
[e]Department of Earth and Marine Science, University of Palermo, Palermo, Italy
[f]Department of Earth Sciences, University of Oxford, Oxford, United Kingdom
Corresponding authors: santiago.arellano@chalmers.se, bo.galle@chalmers.se

Abstract

This report summarizes the findings of plume gas measurements conducted on volcanoes of Papua New Guinea (PNG) during September 2016, as part of the DECADE project. The total sulfur dioxide (SO_2) and carbon dioxide (CO_2) gas fluxes of Tavurvur, Bagana and Ulawun volcanoes were determined by combining ground- remote sensing and ground-/airborne direct sampling, depending on the particular conditions on each volcano. During the campaign Tavurvur was degassing passively, without forming a continuous plume, and it was accessible for direct sampling in the crater. Its SO_2 emission was found to be 0.19 ± 0.05 kg/s from scanning-DOAS and a stationary wide-field-of-view (WFOV) DOAS monitor, and the fraction of CO_2/SO_2 molar ratios was 2.6, obtained with a compact multi-GAS instrument. Bagana, on the other hand, had permanent degassing, producing occasional explosions and ash emission. The plume was measured by ground-based scanning-DOAS and a compact multi-GAS instrument aboard a multi-rotor UAV, resulting in a SO_2 flux of 13 ± 5 kg/s and a CO_2/SO_2 of 15. Ulawun presented continuous passive degassing, forming an elevated plume which flux and composition were measured by car-traverses with a mobile-DOAS, a stationary dual-beam scanning DOAS, and a multi-GAS/UAV sensor. The SO_2 flux of Ulawun was 11 ± 2 kg/s and the CO_2/SO_2 equal to 4.8. A stationary WFOV-DOAS instrument was left with the Rabaul Volcano Observatory (RVO) for longer-term monitoring of the SO_2 flux from Tavurvur.

Keywords: volcanoes of PNG, Tavurvur, Bagana, Ulawun, sulfur dioxide (SO_2), carbon dioxide (CO_2), differential optical absorption spectroscopy (DOAS), multi-component gas analysis system (multi-GAS), unmanned aerial vehicle (UAV), Volcanic Deep Earth Carbon Degassing (DECADE) project

Introduction

Previous studies on volcanic degassing from PNG volcanoes

Papua New Guinea (PNG) is one of the most significant sources of volcanic degassing in the world. Different estimates of the SO_2 emission have been reported in the literature. Andreas and Kasgnoc (1998) ranked Bagana as the second largest source of continuous degassing, after Etna, for the period 1973-1998. The average emission was quantified as 38 kg/s for Bagana, 11 kg/s for Manam, 8kg/s for Langila, and 6 kg/s for Ulawun, all of them between the world's top-11 continuous emitters. Rabaul, most specifically the active volcano Tavurvur, was identified as a sporadic emitter, capable of an output of 301 kg/s during eruptive periods. More recently, a compilation of satellite-based measurements with the OMI sensor (Fioletov et al., 2016) attributes about 15% of the total continuous volcanic emission of SO_2 during the period 2005-2014 to these five volcanoes in Papua New Guinea. Their estimated emissions were of 44 kg/s (Bagana), 17 kg/s (Manam), 8 kg/s (Langila), 7 kg/s (Ulawun), and 22 kg/s (Tavurvur). Focused on the period 2005-2008, McCormick et al. (2012) reported OMI

observations giving a total flux from the PNG volcanoes of 15 kg/s, significantly lower than the previous estimates, which the authors attribute partially to a lower sensitivity of satellite-based measurements and to lower levels of activity. Additionally, McGonigle et al. (2004), conducted mobile-DOAS measurements from an aircraft in July-August 2003 and obtained SO_2 fluxes of 23 kg/s (Bagana), 2.1 kg/s (Manam), 2.9 kg/s (Langila), 7.4 kg/s (Ulawun), 1.3 kg/s (Tavurvur), and 1.4 kg/s (Pago). The local Rabaul Volcano Observatory has, over the last years, conducted measurement campaigns of the SO_2 flux in some of these volcanoes, via traverses with a portable FLYSPEC system (Horton et al., 2006). An estimated of about 3 kg/s of SO_2 has been found for Tavurvur with this method for the period 2009-2014. Through cooperation with the USGS/VDAP, RVO installed a permanent scanning-DOAS (NOVAC) system (Galle et al., 2010) in 2015 at Rabaul to monitor the SO_2 flux from Tavurvur volcano. From the experience gained during the eruptions of Tavurvur between 1994 and 2014, the emission of SO_2 has been regarded as an important indicator of precursory eruptive activity for this volcano (Mulina et al., 2015).

Motivation: to estimate the carbon emission from Bagana, and possibly other volcanoes in PNG

To our knowledge, there are no previous studies of the carbon emission of these highly degassing volcanoes in PNG. Recognizing the expected significance of this volcanic region on the global emission of volcanic carbon, the Volcanic Earth Deep Carbon Degassing (DECADE) program of the Deep Carbon Observatory (DCO) project funded a scientific mission to quantify the emission of carbon from Bagana and other volcanoes in the region.

The role of the Chalmers group was to provide estimates of the SO_2 flux employing remote sensing techniques, which combined with CO_2/SO_2 ratios obtained by our collaborators from Cambridge and Palermo would give the emission rate of CO_2. In consideration of the challenging conditions to access the vent at Bagana for direct sampling of CO_2, Chalmers suggested to attempt deploying a sensor aboard a UAV or drone, and conducted feasibility experiments during the spring of 2016.

Previous experiences with drones for sampling of volcanic plumes have been focused on two categories: small drones capable of transporting payloads lighter than 1 kg up to altitudes of a few hundred meters above ground (e.g., McGonigle et al., 2008) and large, expensive research drones, requiring expert control and special permissions (e.g., Diaz et al., 2010). Chalmers found an alternative portable hexa-copter capable of lifting heavier than 1 kg payloads up to 2 km from ground, with a flight autonomy of about 45 min. These capabilities were demonstrated during tests at the Esrange Space Station in northern Sweden, while training in the use of the drone was conducted at Bo Galle's home in southern Sweden.

The sensor chosen for use with the multi-rotor was loaned from U. Platt's group in Heidelberg University. The system is called Sunkist and it is a compact multi-GAS system suited for use with a drone. The characteristics of the drone and measurement instrument, as well as an in-depth discussion of the methods and results of the CO_2/SO_2 measurements are described in detail in the accompanying report.

Chronology, logistics and measurement conditions

The campaign in PNG lasted from 4 September to 3 October 2016. After arrival, test of instruments and meetings with RVO, the field activities started on 9 Sep. at Tavurvur volcano, then continued at Bagana between 16 and 20 Sep., and finally at Ulawun between 24 and 26 Sep. The last week of the

month was spent in Rabaul working on the installation of a wide-field-of-view (WFOV) DOAS monitor for SO$_2$ flux and on training on NOVAC evaluations and discussions with RVO.

Logistics was greatly facilitated with the help of RVO, who coordinated actions with key local people on each volcano. At Tavurvur, access to the volcano was allowed via RVO, who also provided transport and guiding. To reach Bagana, it is first necessary to fly from Rabaul to Buka, then take a 4-h boat trip to Torokina, a 1.5-h car drive to Gotana, and a 3-to-4-h hike to Wakovi or the foot of the volcano. Transport and guiding/porting was negotiated with RVO contacts. For Ulawun, it is possible to take a 4-h boat trip from Rabaul to Ulamona, or a flight from Rabaul to Hoskins and then a 3-to-4 h car drive to Ulamona. The New West Britain Provincial Disaster Office based at Kimbe provided transport and guiding at Ulawun and volcanoes of the Kimbe area.

Weather conditions were in general good for the purposes of the campaign. At Tavurvur, the main challenge is the high temperature that makes fieldwork extenuating, especially inside the crater. Bagana is in the middle of a rainforest, where tropical rain occurred every day, making impossible to obtain good measurements in the afternoons, and sometimes impeding access through the several rivers that had to be crossed. At Ulawun the conditions were similar to Rabaul, with cloudiness mostly developed from mid-morning and the occurrence of occasional light or heavy but not prolonged rains. Figure 1 shows a georeferenced chronology of the field campaign.
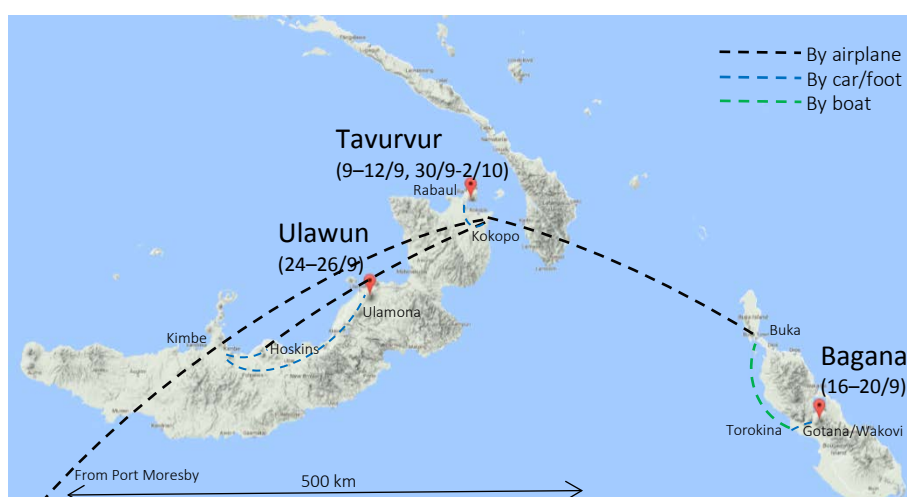
Figure 1. Map showing the locations of some places, means of transport and chronology of the field campaign in PNG

Methods

Scanning-, dual-beam-, WFOV- and mobile-DOAS

Differential Optical Absorption Spectroscopy, DOAS (Platt and Stutz, 2008), is a well-established technique for remote sensing of volcanic gases. In particular, is the method employed for routine SO$_2$ flux monitoring on most volcano observatories in the world, chiefly through the Network for Observation of Volcanic and Atmospheric Change (NOVAC), coordinated by Chalmers (Galle et al., 2010). For this study we employed four configurations of DOAS instruments, scanning-DOAS, dual-beam DOAS, wide-field-of-view DOAS, and mobile-DOAS. All these techniques derive the relative slant-column density of SO$_2$, by a DOAS analysis of a spectrum of skylight from a direction where the volcanic plume is located against a spectrum of skylight from a direction outside of the plume. The analysis is typically done in the 310-325 nm spectral interval and includes the absorption cross-sections of SO$_2$

and O_3, a Ring-effect spectrum, and high-pass filtering to get rid of broad-band structures in the optical depth. Wavelength shift/squeeze is optimized by fitting a solar Fraunhofer spectrum to each spectra, before conversion to transmittance. To get the flux, the column densities are integrated in a cross section of the plume and the integral multiplied by the normal component of plume transport velocity (see Galle et al., 2003; 2010 for details).

Scanning-DOAS consists in a system that scans the plume from a fixed position with a narrow (circular) field of view. We employed a field-campaign, portable instrument described in detail in Conde et al., (2014), which is an adaptation of the system first described in Edmonds et al. (2003). The Dual-beam DOAS is a configuration designed for derivation of the plume speed by cross-correlating two simultaneous time-series of gas column-densities measured at two positions along the plume-axis (Johansson et al., 2009). We employed a portable scanning-DOAS with two channels for this type of measurements. Wide-Field-of-View (WFOV) DOAS consists in a scanning-DOAS with a wide cylindrical field of view, covering the entire cross-section of the plume. It differs from the scanning-DOAS method in that the integration of column densities is done in one spectrum, instead of sequentially. The method is suited for detecting anomalous degassing of dormant volcanoes or weak passive degassing, and it can also be combined with the dual-beam method to estimate the gas emission rate, as described by Boichu et al. (2010). Finally, the mobile-DOAS method consists of a narrow FOV DOAS instrument that produces the integration of vertical column densities by traversing the plume from a moving platform beneath the plume. We did car-traverses with a mobile-DOAS similar to the one first described by Galle et al. (2003). Figure 2a shows some pictures of the DOAS instruments used for this study.

Multi-GAS: Sunkist

To obtain the molar ratios of CO_2 and SO_2 we employed a compact multi-GAS instrument developed by the Institute of Environmental Physics of Heidelberg University, called Sunkist. This instrument comprises a non-dispersive-infrared sensor for CO_2, an electrochemical sensor for SO_2, sensors for temperature, pressure and relative humidity, and a sampling pump. Data collection is controlled by a small computer and power is provided by a 9V alkaline battery. The sampling rate is 0.5 s and the response times of the detectors are lower than 20 s. The instrument weights about 500 g and is compact enough to be carried aboard a UAV. Further specifications are given in the accompanying report, while general details of the multi-GAS technique is given in e.g., Aiuppa et al. (2005) or Shinohara (2005). Figure 2a shows the Sunkist instrument used in this field campaign.

Multi-rotor UAV: Micro

To obtain molar ratios by direct sampling of gases in the plumes of Bagana and Ulawun we tested a portable hexa-copter model Micro, from the SkyEye Innovations company. The characteristics are given in the appended report. This system was for the first time deployed on a volcanic environment, and never before it was used for such high altitudes, higher than 1 km above ground. Tests of the feasibility indicated that with proper batteries an endurance of 45 min and 2 km altitude was achievable with a payload of up to 1.5 kg. Unfortunately, transport of Li-ion or LiPo batteries was not allowed by airplane, and a local provider at PNG was finally not able to provide the proper batteries either. We improvised a solution by making a serial connection of batteries with lower capacity lent by R. D'aleo from S. Aiuppa's group in Palermo. With this arrangement, we could at least obtain an

endurance of about 15 min, which allowed as to make a vertical ascension to the plume for quick sampling and return. Figure 2a shows the drone used in this field campaign.
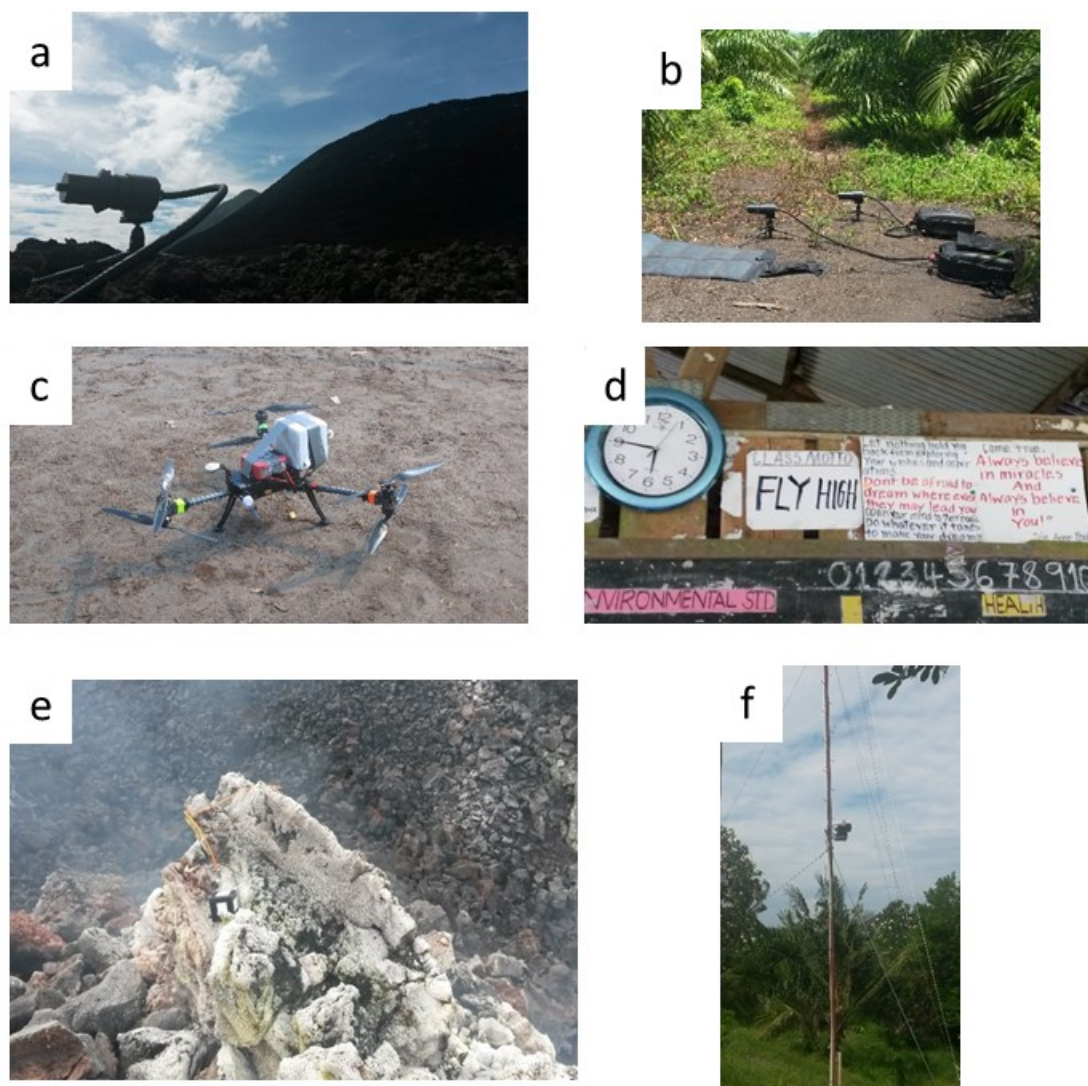
Figure 2a. Photographs of some instruments used in the field campaign in PNG. a) Conical scanning-DOAS instrument measuring the SO_2 flux at Tavurvur; b) parallel measurement with a flat scanning-DOAS and a dual-beam DOAS instruments for SO_2 flux measurements at Ulawun; c) Sunkist (multi-GAS) instrument aboard a Micro (hexa-copter) ready to take-off for measurements of the CO_2/SO_2 ratio in the plume of Bagana; d) Motto of the school at the village of Gotana: "Fly High"; e) Sunkist deployed at the central vent of the crater of Tavurvur; f) installation of a fixed WFOV-DOAS monitor at Matupit, to measure the SO_2 flux of Tavurvur

Figure 2b. Photographs of the volcanoes during September 2016. G) Tavurvur; h) Bagana; i) Ulawun

Sources of meteorological data

When possible, the plume altitude, direction and speed was measured with multiple scanning-DOAS and the dual-beam DOAS techniques. However, in some cases the logistics did not allow to deploy to scanners on the sides of the plume for localization of the plume by triangulation, or the plume itself was not continuous, as required for plume speed measurements. For these cases we determined the plume altitude by visual observation and used this altitude to derive the plume direction by geometrical calculations with a single scanner. In the case of the wind speed, it was retrieved from the ERA interim analysis database of ECMWF (Dee et al., 2011), with a spatial resolution of 0.125/0.125 degree and a time resolution of 6 hours. . In Figure 3 below is shown an example of a dual-beam DOAS plume speed measurement made at Bagana volcano in connection with the drone flight on 20 September 2016, yielding a plume speed of 3.6 m/s.
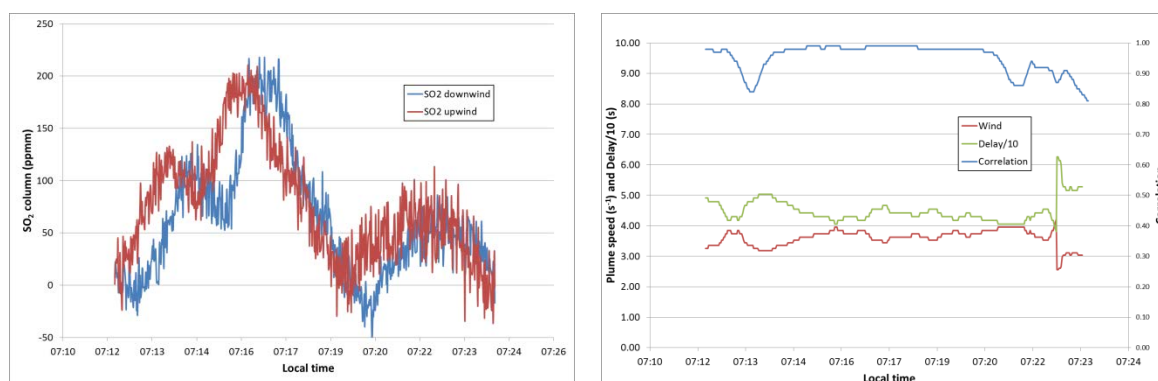
Figure 3. Plume speed measurement made at Bagana on 20 September 2016. (Left): Simultaneous up- and downwind measurements in the plume. (Right): Correlation and time delay between the 2 datasets, giving a derived wind speed of 3.6 m/s

Results

Tavurvur

To estimate the flux of SO_2 at Tarvurvur we setup two scanning-DOAS instruments in the locations depicted in Figure 4. Additionally, we carried out walking traverses with a mobile-DOAS around the base of the volcano (there are no routes in close proximity of the volcano to attempt car-traverses). These traverses were not successful due to the slow measurement of sporadic pulses of emission. We used ECMWF data at the summit altitude for plume speed. The direction of the plume was calculated assuming the gas was drifted at summit altitude.

Figure 4. Map showing the locations of instruments used for measurements of the SO$_2$ flux from Tavurvur. Campaign measurements include temporary deployment of scanning-DOAS (blue circles) and mobile-DOAS traverses (dotted line). Long-term measurements included scanning-DOAS (since 2015) and a WFOV-DOAS instrument installed during the campaign. Data from the stations is transmitted to RVO

We also evaluated the measurements obtained from a monitoring station located at the premises of Hotel Rabaul, about 5 km of Tavurvur. This station was installed in November 2015 by a collaboration between RVO and USGS/VDAP. The recent activity of Tavurvur make measurements from this station quite challenging due to the low emission, altitude of the volcano and distance to the volcano; however, some scans captured the emission from the volcano, as indicated in Figure 5.

Finally, the results of the first month of operation of the WFOV-DOAS instrument installed at Matupit is shown in Figure 5. This instrument is placed at about 2 km distance from Tavurvur and two configurations were tested: single-beam for rapid detection of emission anomalies, and dual-beam for determination of the plume speed. The standard operation mode is the single-beam, from which fluxes are estimated using independent information of the plume direction and speed. The appended report gives details of this technique.
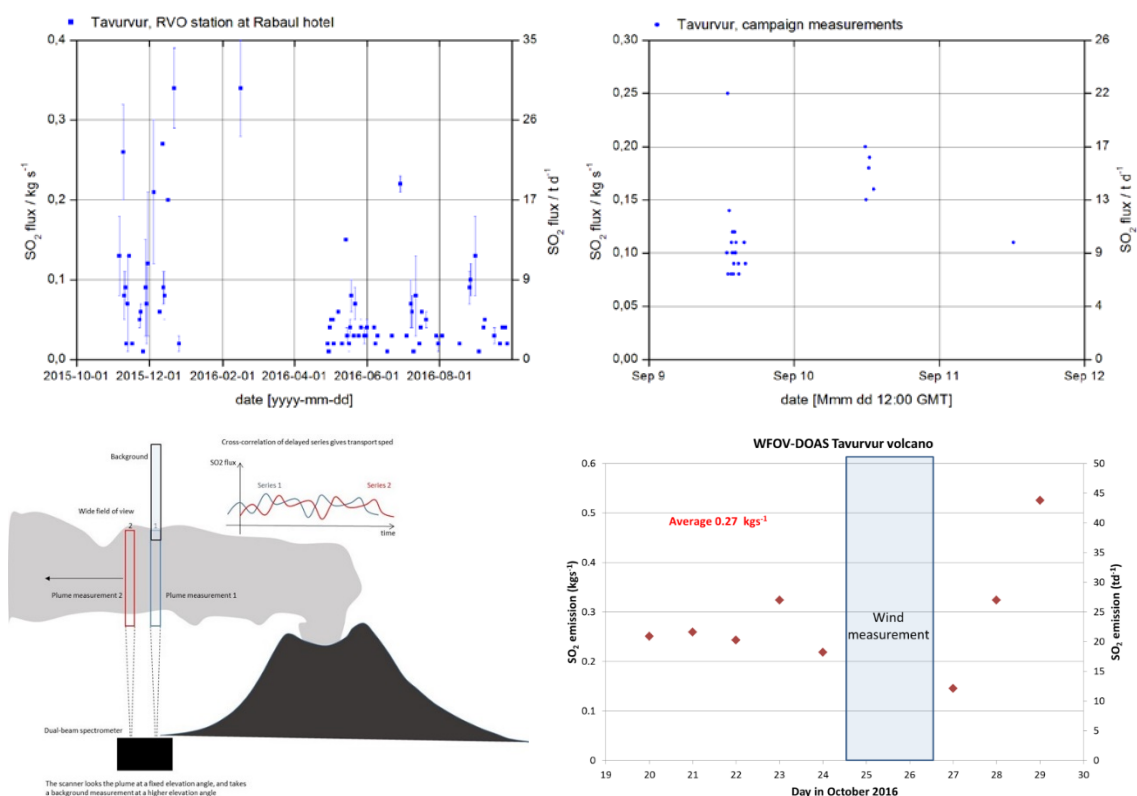
Figure 5. The upper plots show time-series of SO_2 flux measurements at Tavurvur by permanent (left) and temporary (right) scanning-DOAS instruments. The lower plots show the concept of the WFOV-DOAS monitor and a flux time-series for 1 week in October 2016. The remote station measured a mean flux of 0.07 ± 0.07 (mean $\pm$ 1 s.d.) kg/s between November 2015 and October 2016, the campaign measurements gave a flux of 0.12 ± 0.04 kg/s in mid-September, and the WFOV monitor measured a flux of 0.27 ± 0.10 kg/s in end of October 2016

The fraction of molar ratios CO_2/SO_2 was estimated from direct measurements in the central vent inside the crater of Tavurvur. About 45 min are required to reach the crater rim from the base of the volcano, and additional 90 min to access the central vent through a path of unstable erupted products. Details of the method are given in the appended report, and the main results are shown in Figure 6.

9
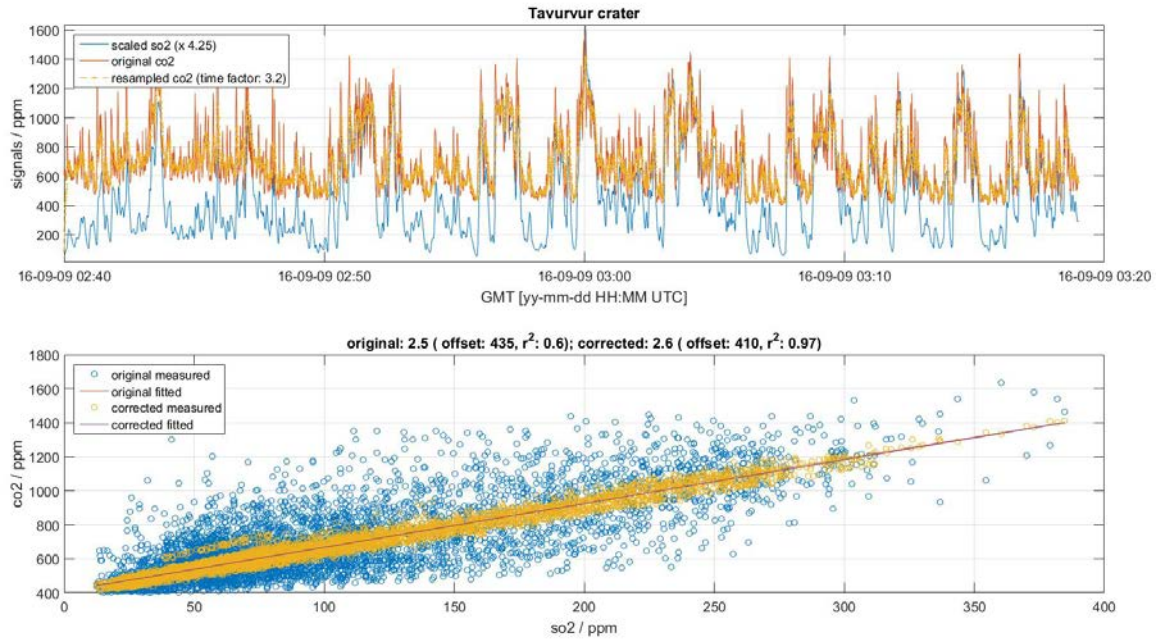
Figure 6. Results of CO_2/SO_2 measurements at the crater of Tavurvur with a Sunkist (multi-GAS) instrument. The upper plot shows the time-series of raw signals of CO_2 (red) and SO_2 (blue, scaled by 4.25), and the signal of CO_2 corrected for time-response. The lower plot shows the scatter-plot of the mixing ratios for the uncorrected (blue) and corrected (yellow) calibrated signals and the linear fit to the plot. The ratio CO_2/SO_2 (molar) was found to be 2.6

Bagana

To measure the SO_2 emission rate from Bagana we attempted walking-traverses with mobile-DOAS that were not completed because of the dense vegetation surrounding the volcano. Scanning-DOAS and dual-beam DOAS were applied successfully from three locations, two at the base of the volcano and over a lahar deposit, and a third one from the village of Wakovi, between about 4.6 and 6.9 km WSW from the volcano. From Wakovi we made two launches of the drone carrying the Sunkist, in parallel to the scanning and dual-beam measurements. Figure 7 shows the locations for measurements and Figure 8 the most important results.

Figure 7. Map showing the location of scanning, dual-beam and mobile-DOAS, and launch site for drone measurements at Bagana
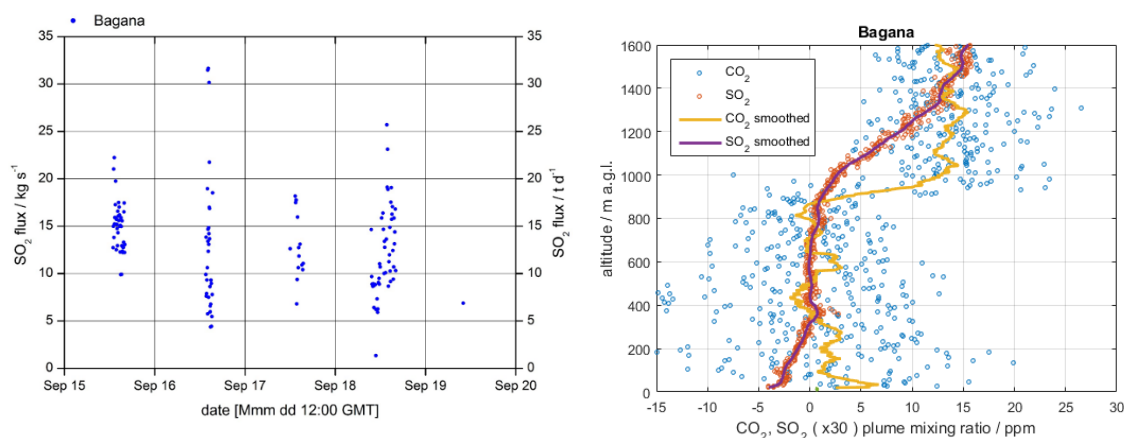

Figure 8. The left plot shows a time-series of SO_2 flux measurements at Bagana by temporary scanning-DOAS and dual-beam DOAS instruments. The mean flux of SO_2 was found to be 13 ± 5 kg/s. The right plot shows the altitude profile of CO_2/SO_2 measurements at the plume of Bagana with a drone/multi-GAS system. The mean CO_2/SO_2 ratio was found to be 15 from the region of maximum plume concentration above the detection limits of the SO_2 sensor

Ulawun

Around Ulawun there is a ring-road and a series of small paths in direction towards the volcano, through dense palm-oil plantations. We conducted mobile-DOAS car traverses from the ring-road and accessed two of the routes to approach sites below the plume for launching of the Sunkist/Micro system. Dual-beam DOAS measurements were done in parallel to determine the plume speed. Figure 9 shows the locations for measurements and Figure 10 the results.

Figure 9. Map showing the location of scanning, dual-beam and mobile-DOAS, and launch site for drone measurements at Ulawun
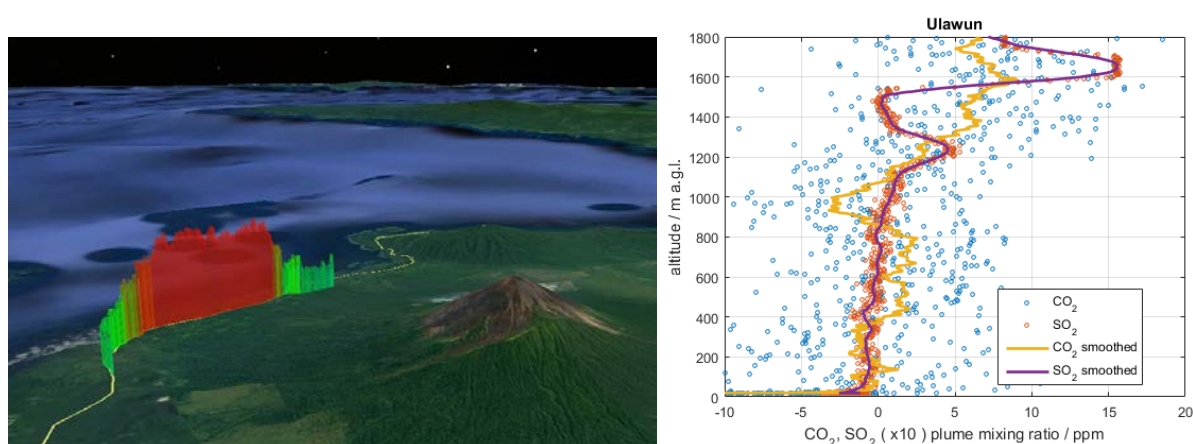
Figure 10. The left plot shows a Google-Earth image of a mobile-DOAS traverse around Ulawun. The mean SO_2 flux from 8 traverses was found to be 11 ± 2 kg/s. The right plot shows the altitude profile of CO_2/SO_2 measurements at the plume of Ulawun, where the molar ratio was found to be 4.8

Conclusions and future work

The volcanoes of PNG offered different challenges for measurement of the gas output. On one hand, accessibility is not always straightforward, as in the case of Bagana; on the other, the emission is weak and intermittent, as in Tavurvur, or weather conditions can change abruptly making the measurements difficult.

By combining different measurement strategies and instruments we were able to characterize the emission of CO_2 and SO_2 from Tavurvur, Bagana and Ulawun during September 2016. To achieve detection of CO_2 at the high plumes of Bagana and Ulawun we tested a direct sampling technique aboard a portable, high-altitude multi-rotor. Such approach opens up several possibilities for volcanic plume studies at high elevation without expert and expensive control, and to the best of our

12

knowledge it has only being previously applied in Japan (Mori et al., 2016). In order to measure the weak emissions from Tavurvur we applied a monitoring strategy with a WFOV-DOAS instrument, which we have also applied in Iceland for early warning of emission anomalies at the volcanoes Hekla and Katla.

Our results indicate that Tavurvur is presently in state of weak passive degassing. Gas is emitted from a central vent and crater fumaroles inside the crater, usually as occasional puffs, without forming a plume. The mean emission of SO_2 for the period November 2015-October 2016 was between 0.1 and 0.2 kg/s, and we estimate a corresponding flux of CO_2 of 0.18 and 0.37 kg/s.

Bagana is currently degassing continuously, mostly from a vent on the upper western flank. The emission is associated with sporadic ash explosions and pyroclastic flows. In spite of this high activity the emission during our field work was lower than that reported in previous years. We estimate a flux of SO_2 of 13 kg/s during September 2016, and a flux of CO_2 of 134 kg/s.

Ulawun is presently degassing passively from an open-vent in the summit, without emission of ash or explosive activity. The plume is continuous and elevates some hundreds of m above the summit. From our observations we derive a SO_2 flux of 11 kg/s and a CO_2 flux of 36 kg/s.

Table 1 summarizes the findings of this campaign, and Figure 11 presents our results in relation to previous studies.

Table 1. Results of the field campaign in PNG. The values correspond to the mean $\pm$ 1 s.d. of variability

Volcano	CO_2/SO_2 ppm/ppm	SO_2 flux kg/s	CO_2 flux kg/s	Techniques	Degassing activity
Tavurvur	2.6	0.19 ± 0.05	0.34 ± 0.09	scanning-DOAS, WFOV-DOAS, direct multi-GAS	Weak passive
Bagana	15	13 ± 5	134 ± 52	Scanning-DOAS, dual-beam DOAS, drone/multi-GAS	Moderate passive/explosive
Ulawun	4.8	11 ± 2	36 ± 6.6	Mobile-DOAS, dual-beam DOAS, drone/multi-GAS	Moderate passive
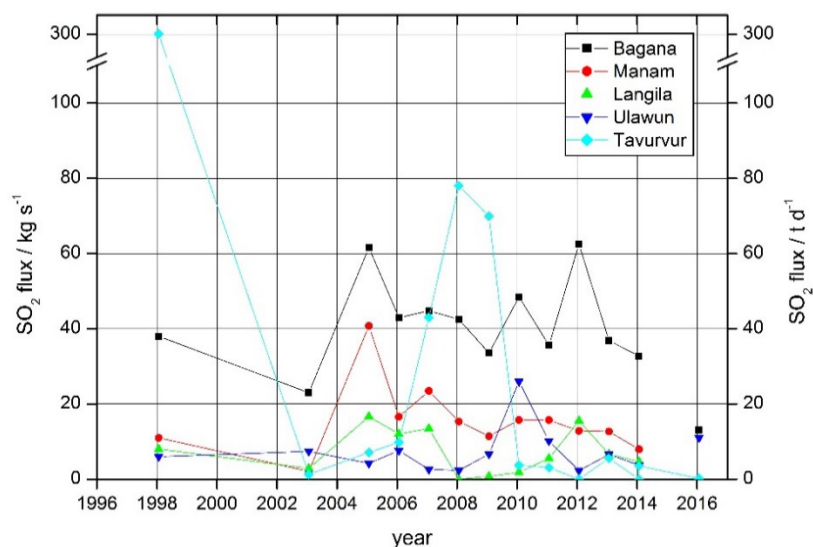
Figure 11. Time-series of mean annual SO_2 flux measurements at PNG volcanoes. Sources of the estimates are: *Andreas and Kasgnoc (1998)* for the period 1973-1998; *McGonigle et al. (2004)* for Jul.-Aug. 2003; *Fioletov et al., (2016)* for the period 2005-2014; *Mulina (2015)* for 2009-2014 (Tavurvur); and this study for the period 2015-2016 (Tavurvur) and Sep. 2016 (Tavurvur, Bagana, Ulawun)

From the experiment with the drone/multi-gas system we found some problems that should be considered in the future. First, we were not able to transport or purchase proper batteries in PNG due to regulations. Well in advance we counted with flight permissions through the support from RVO, however, it is not possible to transport the required batteries in commercial flights and a local provider could not get the batteries, as we had been promised. This resulted in a serious limitation in the time of measurement achieved by improvising a solution with available batteries. With proper power it would have been possible to sample the plume for longer time, avoiding problems with the sensors. Second, we did a first attempt of measurement with the Sunkist system aboard a drone, and found some uncertainties regarding stability of the sensors.

In the future we will keep collaborating with RVO on the ongoing monitoring activities with our installed WFOV instrument and the NOVAC station installed by VDAP. We envision further work on the interesting volcanoes of PNG, possibly including Manam or Langila in a future visit.

References

Aiuppa, A., C. Federico, G. Giudice, and S. Gurrieri, Chemical mapping of a fumarolic field: La Fossa Crater, Vulcano Island (Aeolian Islands, Italy), Geophys. Res. Lett*.*, 32, L13309, doi:10.1029/2005GL023207, 2005.

Andres, R. J*., and* Kasgnoc A.D. (1998), A time-averaged inventory of subaerial volcanic sulfur emissions, J. Geophys. Res., 103(D19), 25251–25261, doi:10.1029/98JD02091*.*

Boichu, M., Oppenheimer, C., Tsanev, V.I. & Kyle, P.R, (2010), High temporal resolution SO_2 flux measurements at Erebus volcano, Antarctica, Journal of Volcanology and Geothermal Research, 190, 325-336, doi:10.1016/j.jvolgeores.2009.11.020.

Conde, V., Nilsson, D., Galle, B., Cartagena, R., and Muñoz, A.: A rapid deployment instrument network for temporarily monitoring volcanic SO_2 emissions – a case study from Telica volcano, Geosci. Instrum. Method. Data Syst., 3, 127-134, doi:10.5194/gi-3-127-2014, 2014.

Dee, D. P., Uppala, S. M., Simmons, A. J., Berrisford, P., Poli, P., Kobayashi, S., Andrae, U., Balmaseda, M. A., Balsamo, G., Bauer, P., Bechtold, P., Beljaars, A. C. M., van de Berg, L., Bidlot, J., Bormann, N., Delsol, C., Dragani, R., Fuentes, M., Geer, A. J., Haimberger, L., Healy, S. B., Hersbach, H., Hólm, E. V., Isaksen, L., Kållberg, P., Köhler, M., Matricardi, M., McNally, A. P., Monge-Sanz, B. M., Morcrette, J.-J., Park, B.-K., Peubey, C., de Rosnay, P., Tavolato, C., Thépaut, J.-N. and Vitart, F. (2011), The ERA-Interim reanalysis: configuration and performance of the data assimilation system. Q.J.R. Meteorol. Soc., 137: 553–597. doi:10.1002/qj.828.

Diaz J., Pieri D., Arkin C., Gore E., Griffin T., Fladeland M., Bland G., Soto C., Madrigal Y., Castillo D., Rojas E., Achí S. (2010) Utilization of in situ airborne MS-based instrumentation for the study of gaseous emissions at active volcanoes, Intern. J. Mass. Spectrom., 295:3, 105-112.

Edmonds, M., Herd, R.A., Galle, B., Oppenheimer C., Automated, high time-resolution measurements of SO_2 flux at Soufrière Hills Volcano, Montserrat, Bull Volcanol (2003) 65: 578. doi:10.1007/s00445-003-0286-x.

Fioletov V., McLinden C., Krotokov N., Li C., Joiner J., Theys N., Carn S., Moran M., A global catalogue of large SO_2 sources and emissions derived from the Ozone Monitoring Instrument, Atmos. Chem. Phys., 16, 11497–11519, 2016, doi:10.5194/acp-16-11497-2016.

Galle B., Oppenheimer C., Geyer A., McGonigle A., Edmonds M., Horrocks L., A miniaturised ultraviolet spectrometer for remote sensing of SO_2 fluxes: a new tool for volcano surveillance, J. Volcanol. Geotherm. Res., 119, 1–4, 2003, 241-254, doi:10.1016/S0377-0273(02)00356-6.

Galle, B., Johansson M., Rivera C., Zhang Y., Kihlman M., Kern C., Lehmann T., Platt U., Arellano S., and S. Hidalgo (2010)*,* Network for Observation of Volcanic and Atmospheric Change (NOVAC)—A global network for volcanic gas monitoring: Network layout and instrument description, J. Geophys. Res., 115 D05304, doi:10.1029/2009JD011823*.*

Horton, K. A., Williams-Jones G., Garbeil H., Elias T., Sutton A. J., Mouginnis-Mark P., Porter J. N., Clegg S., Real-time measurement of volcanic SO_2 emissions: Validation of a new UV correlation spectrometer (FLYSPEC), Bull. Volc. 68: 4, 323-327, 2006a, DOI 10.1007/s00445-005-0014-9.

Johansson, M., Galle, B., Zhang, Y., Rivera C., Cheng D., Wyser K., The dual-beam mini-DOAS technique—measurements of volcanic gas emission, plume height and plume speed with a single instrument, Bull Volcanol (2009) 71: 747. doi:10.1007/s00445-008-0260-8.

McCormick, B. T., Edmonds M., Mather T*.,* Carn S. (2012), First synoptic analysis of volcanic degassing in Papua New Guinea, Geochem. Geophys. Geosyst., 13, Q03008, doi:10.1029/2011GC003945*.*

McGonigle, A. J. S., Oppenheimer C., Tsanev V.I., Saunders S., Mulina K., Tohui S., Bosco J., Nahou J., J. Kuduon, and Taranu F. (2004)*,* Sulphur dioxide fluxes from Papua New Guinea's volcanoes, Geophys. Res. Lett., 31, L08606, doi:10.1029/2004GL019568*.*

McGonigle A. J. S., Aiuppa A., Giudice G., Tamburello G., Hodson A.J., Gurrieri S., (2008), Unmanned aerial vehicle measurements of volcanic carbon dioxide fluxes, Geophys. Res. Lett., 35, L06303, doi:10.1029/2007GL032508.

Mori, T., Hashimoto, T., Terada, A., Yoshimoto, M., Kazahaya, R., Shinohara, H. & Tanaka, R. (2016). Volcanic plume measurements using a UAV for the 2014 Mt. Ontake eruption. Earth, planets and space 68, 49.

Mulina K., Monitoring SO_2 emissions from Tavurvur volcano, Rabaul, PNG, Presentation at the 5th NOVAC Workshop, Costa Rica, 2015.

Platt U., Stutz J., Differential absorption spectroscopy, differential optical absorption spectroscopy, Physics of Earth and Space Environments, Springer, Berlin Heidelberg (2008).

Shinohara, H., A new technique to estimate volcanic gas composition: Plume measurements with a portable multi-sensor system, J. Volcanol. Geotherm. Res., 143, 319–333, 2005.

Annexes

Arellano S., Galle B., Direct CO_2/SO_2 plume measurements in Papua New Guinea with a drone-based Micro-Sunkist system – Fieldwork report, Chalmers University of Technology, 17 p.

Arellano S., Galle B., Wallius J., K. Mulina, I. Itikarai, J. Bosco, Ezequiel, New concept for gas monitoring of Tarvurvur volcano, PNG: Wide field of view-dual beam scanning DOAS - Installation report, Chalmers University of Technology, 10 p.

Direct CO₂/SO₂ plume measurements in Papua New Guinea with a drone-based Micro-Sunkist system

Santiago Arellano, Bo Galle
Department of Earth and Space Sciences,
Chalmers University of Technology, SE-41296 Gothenburg, Sweden
santiago.arellano@chalmers.se; bo.galle@chalmers.se

Abstract

This report summarizes the findings from the drone-based measurements with a compact CO_2 and SO_2 sensors system in the plumes of Tavurvur, Bagana and Ulawun volcanoes in Papua New Guinea, obtained during September 2016. Molar ratios for CO_2/SO_2 of 2.6, 15 and 4.8 were found for these volcanoes, respectively.

1. Introduction

Within the framework of the DECADE/DCO project, Chalmers participated in a field campaign in Papua New Guinea (PNG) between 6 September and 3 October 2016. The main goal of the campaign was to obtain estimates of the carbon dioxide (CO_2) output from Bagana (1750 m a.s.l.) and other strong degassing volcanoes in PNG. While volcanic sulfur dioxide (SO_2) can easily be measured from ground by remote sensors, CO_2 is more challenging due to the high atmospheric abundance of this species, making direct sampling of the volcanic plume necessary. Due to the high level of activity and high altitude of Bagana volcano, is not possible to access the crater or volcanic plume for manual direct sampling, therefore we attempted measurements with a high-altitude drone system capable of lifting a compact MultiGAS-type instrument for unmanned aerial sampling of the plume.

While the concept of sampling with a UAV-based sensor has been tried before (cf. References), previous studies use either small commercial drones suitable for low-altitude plumes or high cost, sophisticated research UAVs, which can endure long distances and altitudes but require expert operation. Measurements at high elevation with small, easily controlled drones have only been attempted, to our knowledge, by Mori et al. (2016) to measure the emissions from Mt. Ontake in Japan at an altitude of about 1000 m above ground with a set of sensors onboard a commercial eight-propeller drone.

Our solution consisted on equipping a powerful but simple hexa-copter (six-propeller drone) with a compact CO_2/SO_2 sensor in combination with standard scanning-DOAS measurements of SO_2 from ground. Tests and training on the use of the drone were done in open-areas and the Esrange Space Center (ESC) in northern Sweden during the summer of 2016. These tests probed the feasibility to lift a payload of up to 1.5 kg to an altitude of 2000 m above ground, beyond which radio control is usually lost. The tests also characterized the power consumption and speed, and manual or auto-pilot flying modes of the drone. A suitable, compact gas sensor has been already developed by L. Tirpitz from N. Bobrowski and U. Platt group in Germany, which was lent for our measurements conducted in PNG.

2. Micro-Sunkist system

The drone was hired from the Swedish company SkyEye Innovations, the model is called Micro (http://skyeyeinnovations.se/start/airborne-solutions/sky-eye-micro/). This drone is normally used

for thermal surveillance in video at low elevations so it was necessary to test the system with typical payloads and altitudes required for volcanic studies. Figure 1 below shows the current consumption measured during test in the ESC near Kiruna with a payload of 800 g. The typical consumption during ascent was about 50 A, 33 A for hoovering, and 20 A for descent. With a Li-ion battery pack with 25Ah capacity, it is then possible to achieve about 45 minutes of round flight even with relatively strong winds. The navigation system of the drone makes possible to plan a flight mission, as well as to activate several emergency return or landing options if necessary. The drone weights about 7 kg (without case and batteries) and it is foldable and easy to transport. It uses 3 pairs of propellers and radio-control for a typical range of 2-2.5 km.
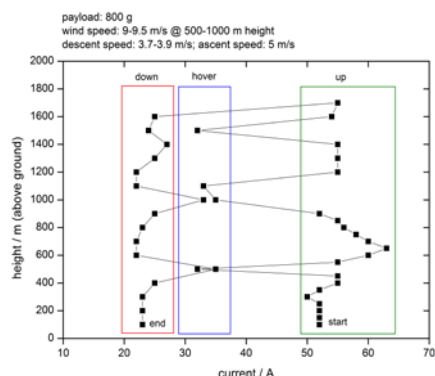
Figure 1. –left– Charge consumption measured with the SkyEye Micro drone in a high-altitude test with a payload similar to the gas sensor for volcanic plumes. –right– The Micro+Sunkist system ready to take-off at Bagana. The Sunkist is inside a fabrics box with the inlet pointing in direction of the drone's nose. The Li-ion battery pack is behind the Sunkist. The total payload should be placed to keep the centre of mass equidistant to the rotor pairs. Behind the batteries the GPS and communication antennas are shown, as well as the power connector (unplugged) behind the batteries

A critical consideration is the choice of batteries. We tested both Li-ion and LiPo battery packs with a capacity of 25Ah and a voltage of 24V. The former are heavier but less flammable, however both types present restrictions for transport by airplanes, and even have some embargo for use in some countries, including PNG. Further characteristics of the Micro drone are given in Table 1.
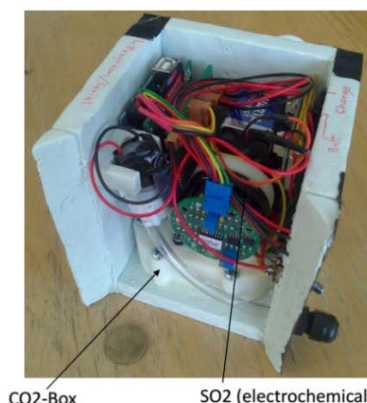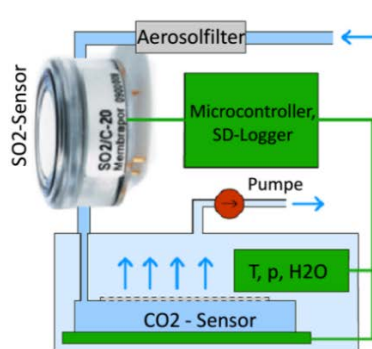
Figure 2. Sketch and photograph of the Sunkist sensor for in-situ measurement of volcanic CO_2 and SO_2 concentrations. The instrument is protected by a foam case and has one power switch, one gas inlet and one gas outlet. The acquisition is controlled by a microcomputer and data is saved in text format in a micro-SD card. Besides the CO_2 and SO_2 sensors, there is a pump, a thermometer, a barometer, and a hygrometer. The computer has a USB-chargeable battery and the sensors are powered by a 9V alkaline battery (images courtesy of L. Tirpitz)

The gas sensor developed by the N. Bobrowski and U. Platt group is called Sunkist and it was designed for use in volcanic measurements. The system is ideal for this application, given its robustness and compact design. The system was sent directly for the campaign and used in the field, and laboratory calibration measurements were done after return to Sweden. The characteristics of the drone and gas sensor are given in Table 1.

Table 1. Characteristics of the Micro-Sunkist system (http://skyeyeinnovations.se/start/airborne-solutions/sky-eye-micro/)

Micro drone	
Operating height	2600 m
Operating temperature	-30 to 50°C
Operating speed	Up to 15 m/s
Rate of climb	Up to 6 m/s
Maximum thrust	120 N
Recommended payload	500 g
Tested payload	1500 g
Power	25Ah, 24V (6S/4P Li-ion battery pack)
Dimensions	80×20×23 cm (Diameter×H×W)
Flying modes	Manual, auto-pilot
Flight information	Altitude, row/pitch/roll angles, speed, power
Sunkist sensor	
CO_2 sensor	NDIR, SenseAir CO2 Engine K33 FR
SO_2 sensor	Electrochemical, CiTiceL 3MST/F
Operating temperature	0−50°C (CO_2), -20−50°C (SO_2)
Operating humidity	0−95% (CO_2), 15−90% (SO_2), non-condensing
Operating pressure	Atmospheric ± 10% (SO_2)
Temperature dependence	1/T (assumed for CO_2), 0.25%/°C (SO_2)
Pressure dependence	1.6%/kPa (CO_2), 0.0015%/kPa (SO_2)
Gas interference	Not declared or not important
Response time	2 s (CO_2), <20 s (SO_2)
Accuracy	±30 ppm ± 3% signal (CO_2), ± 1% signal (SO_2)
Resolution	0.5 ppm (SO_2)
Range	0−5000 ppm (CO_2), 0−200/500 ppm (SO_2)
Warm-up time	1 min (CO_2)
Other sensors	Temperature, pressure, relative humidity
Computer	Arduino, with microSD card for data storage
Voltage	9V (from alkaline battery), about 10 h autonomy
Sampling rate	2 Hz
Weight	500 g
Dimensions	14×13×14 cm (L×W×H)

3. Measurements

Calibration

A few days after returning from the field, a laboratory calibration was performed to determine the response of the Sunkist sensors to know concentrations of gases. We used a mixture of CO_2 and SO_2 at nominal concentrations of $4.293 \pm 0.086\%$ (mol) and 203.9 ± 4.1 ppm (mol), respectively (i.e. in a ratio of 210.5:1), and mix it with pure N_2 to prepare diluted mixtures at 0, 0.5, 1, 2, and 4 ppm SO_2. The mixture was controlled by a dynamic gas calibrator (Thermo Scientific, model 146i) with a flow rate of 5 l/min. The mixture was pumped into the inlet of the Sunkist at a constant flow rate of 0.5 l/min and ambient temperature (27.8°C) and pressure (102 kPa). Each mixture was measured for periods of about 20 minutes after the gas calibrator was stabilized. One week later, the instrument was returned

to Heidelberg/Mainz, where independent calibrations were done. The results presented in this report are based in these last calibrations. Coefficients of the calibration curves are shown in Figure 3 and Table 2 below.
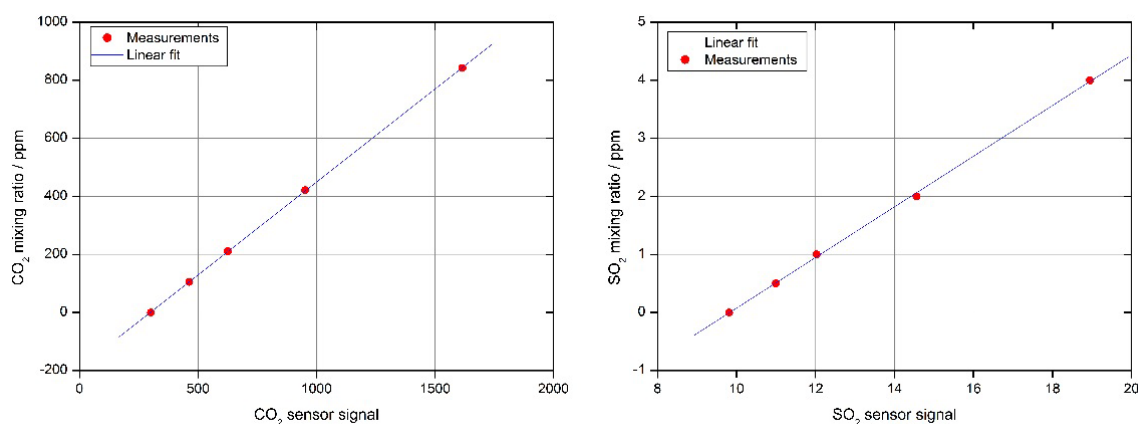
Figure 3. Results of the calibration of the CO_2 –left– and SO2 –right– sensors of the Sunkist system performed in Gothenburg. The instruments show linear behavior in the range of gas mixing ratios relevant to volcanic conditions. The precision of the ordinates and abscissas are smaller than the sizes of the dots

Table 2. Calibration constants for the gas sensors in the Sunkist. The conditions during the calibration were: $27.8 \pm 0.2°C$ (temperature); 102.032 ± 0.033 kPa (pressure); $9.71 \pm 0.19\%$ (relative humidity), as measured by the sensors of the instrument. The R^2 value of the regression is >0.999 for both sensors.

Sensor	Gothenburg		Heidelberg/Mainz	
	Sensitivity	**Offset**	**Sensitivity**	**Offset**
	ppm per reading unit	**ppm**	**ppm per reading unit**	**ppm**
CO_2	$0.65 \pm 0.00(3)$	-191.24 ± 1.28	0.695	-237.8
SO_2	0.43 ± 0.01	-4.29 ± 0.03	0.755	-6.8

Measurements

Instruments were transported to PNG by airplane and tested upon arrival in Rabaul. With the aim of testing the functioning of the Sunkist, it was first deployed for measurements inside the crater of Tavurvur volcano. After testing of the drone, the Micro+Sunkist system was used for measurements at Bagana and Ulawun volcanoes. A map showing the location of these volcanoes and photographs of the measurements with the Micro and Sunkist instruments are shown in Figure 4.
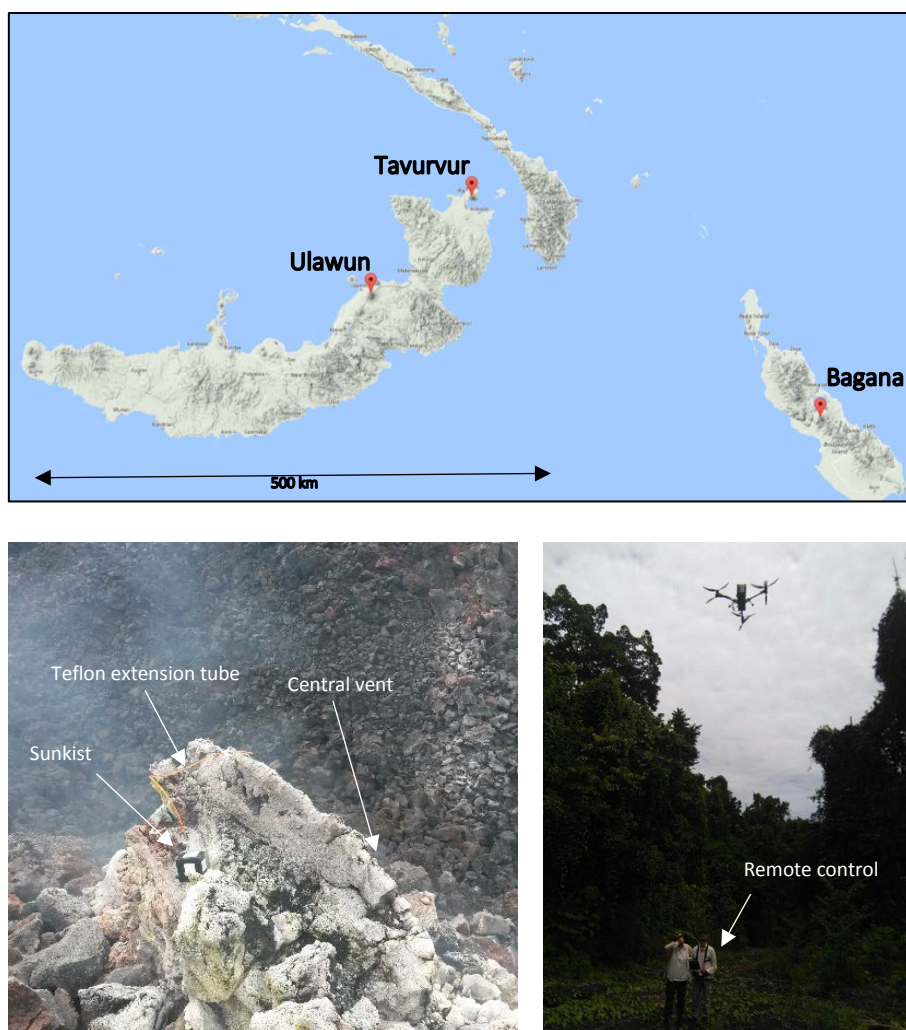
Figure 4. –above– Map showing the location of the volcanoes in PNG that were part of this study (source Google). –below– Photographs of the Sunkist sampling the main vent of Tavurvur and of a Micro-Sunkist measurement on Ulawun

Tavurvur

Tavurvur (-4.239N, 152.21E, 223 m asl) is a cinder cone andesitic volcano, the only presently erupting vent of the Rabaul caldera, in West New Britain. It has produced several explosive eruptions, most notably in 1937, 1994 and 2014. The eruption in 1994 destroyed a large part of the city of Rabaul and the eruption in September 2014 emitted large amounts of ash that disrupted air traffic and reached the stratosphere. Presently Tavurvur exhibits quiescent degassing, with no ash. The emissions of gas tend to accumulate inside the crater and then get released sporadically to the atmosphere. There is a central vent but also fumaroles along the crater walls and floor, in general at non-magmatic temperatures.

Measurements were done on three points inside the crater on 9 September 2016. Weather was good, with occasional clouds and mild winds, but precipitation has occurred a few hours prior the measurements producing steaming through the crater rocks. Two fumaroles were sampled for several minutes by using a teflon tube and a particle filter connected to the inlet of the Sunkist, the first fumarole on the northern side of the crater wall and the second close to the northern edge of the crater floor. A third sampling was done on the central vent (Figure 4).

Bagana

Bagana (-6.14N, 155.195E, 1750 m asl) is probably the most active volcano of PNG. Located in central Bougainvillle Island, about 19 km northeast of the small town of Torokina. It has been more or less active since its first description at the end of the nineteen century, producing some explosive and several effusive eruptions. The most recent activity is characterized by the generation of andesitic lava flows from the central and adventitious vents, as well as secondary lahars triggered by the heavy precipitation in the area. During the last years it has been identified as one of the strongest sources of SO_2 in the world.

There is a persistent emission of gases and varying amounts of ash, which frequently causes disruption in air traffic. We approached the volcano from the southewestern side, and did measurements from the base of the volcano and the nearby village of Wakovi using scanning DOAS and the Sunkist aboard the drone. Weather conditions were usually good early in the mornings and switched to cloudy and rainy around noon.

Ulawun

Ulawun (-5.05N, 151.33E 2334 m asl) is an andesitic stratovolcano located in West New Britain. It is the highest volcano in PNG, surrounded by a very populated area and a strong emitter of SO_2. The present activity is dominated by passive degassing, with rare emission of ash.

Our measurements at this volcano include remote sensing with scanning and mobile DOAS and direct sampling with the Sunkist+drone system. There are several villages around the volcano and a roads surrounding the volcano, but the crater is not accessible.

Details of the raw signals collected on the three volcanoes are presented in Annex I.

4. Analysis

Obtaining mixing ratios from raw signals

The CO_2 sensor in the Sunkist is a non-dispersive infrared detector, which responds to the actual concentration of the target gas, not to its mixing ratio. The SO_2 sensor, on the other hand, is an electrochemical sensor whose output is directly related to the mixing ratio (while the concentration is proportional to pressure, the diffusivity of the transport membrane is inversely proportional to pressure, cancelling the effect). Therefore, in order to obtain the mixing ratio of both molecules and their ratio, the signal from the CO_2 sensor should be compensated for the effects of pressure and temperature. According to the manufacturers' datasheets both sensors present a (very small) sensitivity to pressure (cf. Table 1), but not to temperature or humidity (within the range of operation of the instrument). For the CO_2 sensor, we interpret this dependency as the combined effect of gas expansion (ideal gas law) and possibly broadening of the absorption lines due to pressure. Thus, the raw signals for each molecule S_A (where A represents CO_2 or SO_2) obtained at conditions P, T were either compensated with the datasheet coefficients or scaled to laboratory conditions P_0, T_0, assuming ideal-gas behavior, and then converted to mixing ratio units by using the calibration sensitivity $\frac{\Delta X_A}{\Delta S_A}$ and offset X_A^{offset} coefficients taken at room temperature, i.e.:

$$X_{CO_2} = \left[S_{CO_2} \left(\frac{\Delta X_{CO_2}}{\Delta S_{CO_2}} \right)_0 + \left(X_{CO_2}^{offset} \right)_0 \right] \frac{P_0 T}{T_0 P} \qquad (1a)$$

$$X_{SO_2} = \left[\frac{S_{SO_2}}{1 + \left(\frac{\delta S_{SO_2}}{\delta P} \right)(P - P_0)} \right] \left(\frac{\Delta X_{CO_2}}{\Delta S_{CO_2}} \right)_0 + \left(X_{SO_2}^{offset} \right)_0 \qquad (1b)$$

The laboratory temperature and pressure are given in the section on Calibration. For each individual measurement the temperature scaling was done using the mean temperature of the respective dataset in the case of the crater measurements or using a temperature gradient of -6.5 K/km. We did not use the individual internal thermometer readings because they seem not to correspond to the sample temperature, as it can be seen in the raw data plots in Annex I. On the other hand, pressure correction was done using the individual pressure sensor readings, as they follow a normal trend.

Response time correction

There are different considerations regarding the sampling of the signals. First, there is of course the Nyquist limit that indicates that fluctuations in the input with a frequency higher than at least half of the sampling frequency will not be reproduced faithfully. In our case, this limit corresponds to fluctuations in the input quicker than 1 Hz. Measurements taken close to a hot vent may be highly turbulent, producing quick changes in the mixing with air; however, a change in the actual ratio of molar concentrations of the magmatic species, which is the quantity of interest, is not expected within the sampling period, nor even the entire measurement session. The mixing ratio fluctuations in the more distant plumes are much less attenuated. We conclude that the sampling frequency is not a problem in these measurements.

Both gas sensors have different time responses, being the optical CO_2 sensor faster than the electrochemical SO_2 sensor. Datasheets of the fabricants (Table 1) state that the CO_2 sensor has a time response of 2 s at the flow rate of the instrument, and of <20 s for the SO_2 sensor. The effect of different time responses is twofold: the amplitudes of the signals will be lower than the amplitudes of the inputs and there will be a time shift in the signals. If not corrected for, the first effect may translate in an error in the molar ratios, while the second will normally produce a dispersion in the scatter-plot of the two signals.

We applied a correction for the different time responses assuming that both sensors have a first-order response, which means that their transfer functions have the same functional form and depend on the sensitivities and time responses only. We then iteratively modify the transfer function of the faster instrument (CO_2) until an optimal correlation between the two signals is found. This is equivalent to resample the 'fast' signal with the time response of the 'slow' signal, keeping the same sensitivities. Thus, although the actual time responses are not derived, their relative factor is found. This factor will be closer to the true factor of time responses when the signal is highly variable, i.e. when the input is closer to an impulse. An example of the method applied on the measurements at the vent of Tavurvur is shown in Figure 5.
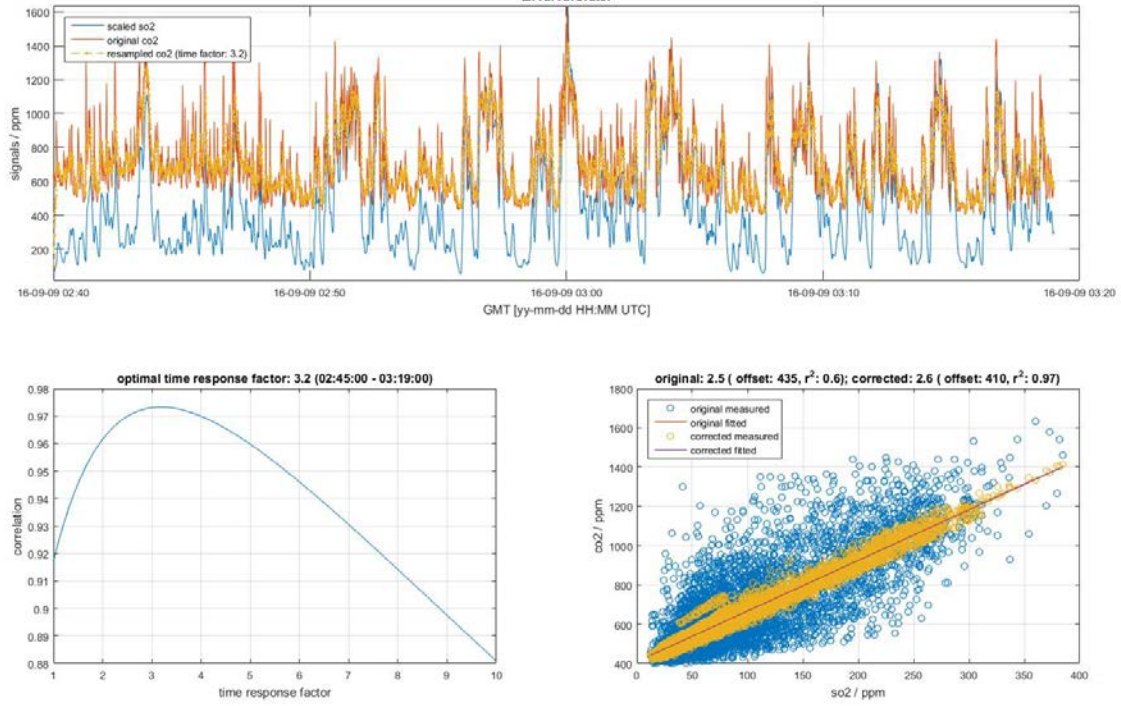
Figure 5. –above– Section of the measurement in the crater of Tavurvur showing the original CO_2 (red) and SO_2 (blue, scaled to CO_2) signals, and the resampled CO_2 signal (orange) at the optimal time response factor. – below– On the left the mapping of the correlation of the two signals at different time response factors. A value of 3 is found to be optimal. On the right the scatter plot of the two signals, before (blue) and after (orange) the correction. Note the important reduction in variance between the two signals

Water mixing ratio and altitude estimation

From the ancillary measurements of the Sunkist of temperature, pressure and relative humidity it is possible to estimate both the mixing ratio of H_2O and the altitude of the measurement (in the case of drone flights). For the first, we used 2 different analytical approximations which give nearly identical results. The most compact is due to Jensen (1990), which gives in ppm:

$$X_{H_2O} = 61.365 RH e^{\left(\frac{17.502\,T}{240.97+T}\right)} \tag{2}$$

Where RH represents the percentage of relative humidity and the temperature is T is expressed in °C. The mixing ratio of H_2O cannot be attributed to the volcanic component only from its ratio to SO2, since the background mixing ratio can be comparable to the volcanic mixing ratio (see details below).

For estimates of the altitude, as it can be seen in the raw pressure plots of Annex I, the ascent took shorter than the descent of the drone. This is compatible with measurements taken during the flight tests (Figure 1), which indicated that ascent was done at typical speeds of 5+ m/s, while descent seems to be set to a maximum of 4 m/s. Assuming that the latter speed was achieved during descent, the ascent speed can be derived from the duration of ascent, or vice versa. The altitude can then be estimated from the pressure measurements, based on the barometric formula. First, the maximum altitude is found by simply using the constant speed and time of descent. From this, the atmospheric scale height is found by inverting the barometric formula between the minimum and maximum pressures measured by the sensor, and then the altitude for each data point is found from:

$$h(P) = h_0 + \bar{h} ln\left(\frac{P_0}{P}\right) \tag{3}$$

8

Where P is pressure, h_0 a reference height of 20 m above ground level (from where the steady ascent started), $\bar{h}$ is the scale height found between the initial and minimum pressures, and P_0 is the pressure at the reference height.

Data selection

Before analyzing the molar ratio between the two molecules, filters were applied to discard data points taken outside of the range of operation in temperature, pressure and relative humidity of the sensors, which are shown in Table 1.

Molar ratio calculation

After compensation for pressure effects, application of the calibration constants, correction of different time responses and data validation, the molar ratio of the species was taken by two different methods. For the measurements inside the crater of Tavurvur a linear fit to the scatter plot of CO_2 vs. SO_2 was applied, giving as offset the background concentration of CO_2 and as slope their molar ratio CO_2/SO_2. As example of this method to the measurements at the vent is shown in Figure 6. For the measurements with the drone, it was found that the background mixing ratios presented gradients with altitude. The cause of this is unknown, but may be due to the rather extreme conditions of measurements, in the tropical rainforest, close to the sea, or to non-corrected instrument drifts. We decided to subtract to the measured signals linear gradients taken outside of the plume, where the location of the plume was given by the observed changes of trend in the raw signals. Then the ratio of molar mixing ratios was taken as the ratio of areas under the regions or maximum concentration of the plume. Examples of this method on the measurements at Bagana and Ulawun are found in Figure 7 and Figure 8. It can be shown that by applying these methods, the estimated molar ratio of CO_2 vs. SO_2 is lower than the actual molar ratio by a factor $\left(1 - X_{CO_2}^{air}/X_{CO_2}^{source}\right)$, where $X_{CO_2}^{air}$ is the air background mixing ratio of CO_2 (~400 ppm), and $X_{CO_2}^{source}$ is the mixing ratio of a pure sample of magmatic gases (~10^{-2}-10^{-1}). This 'error' is negligible for the CO_2-SO_2, while it may be quite high for species with high background, e.g. H_2O-CO_2.
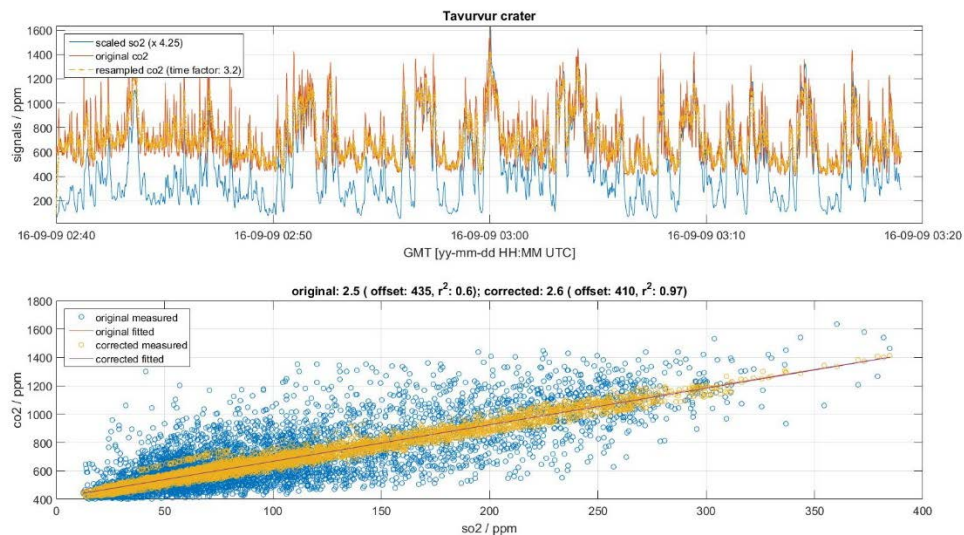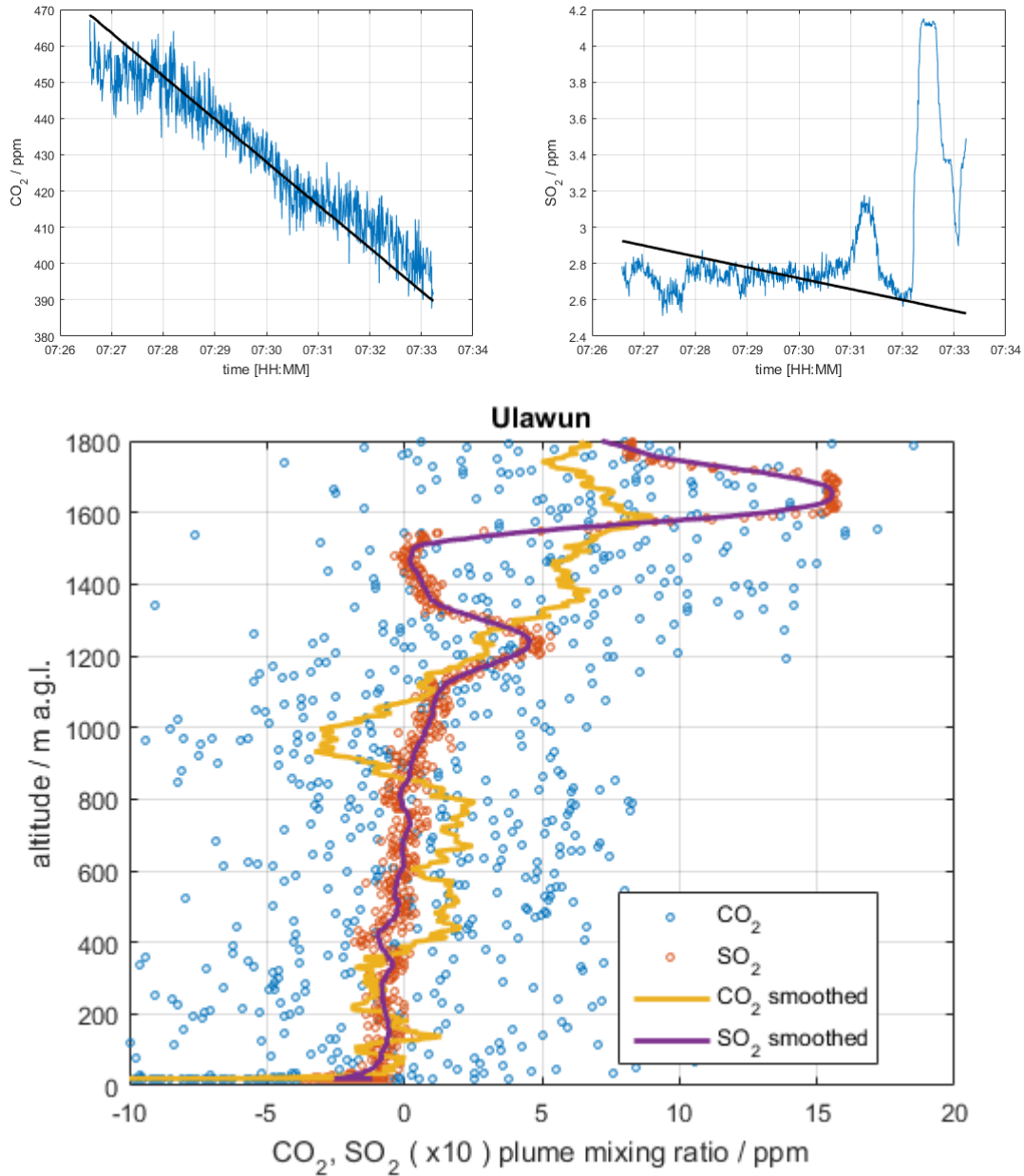

Figure 6. Results of the analysis of the measurement set from the Tavurvur central vent. The upper plot show the original time series for CO_2 (red) and SO_2 (blue, scaled to CO_2) calibrated mixing ratios and the re-sampled CO_2 signal to compensate the slower response of the SO_2 sensor (orange). The lower figures show the CO2-SO2 scatter plot for the original (blue) and resampled (orange) data points, as well as their respective regression lines

9
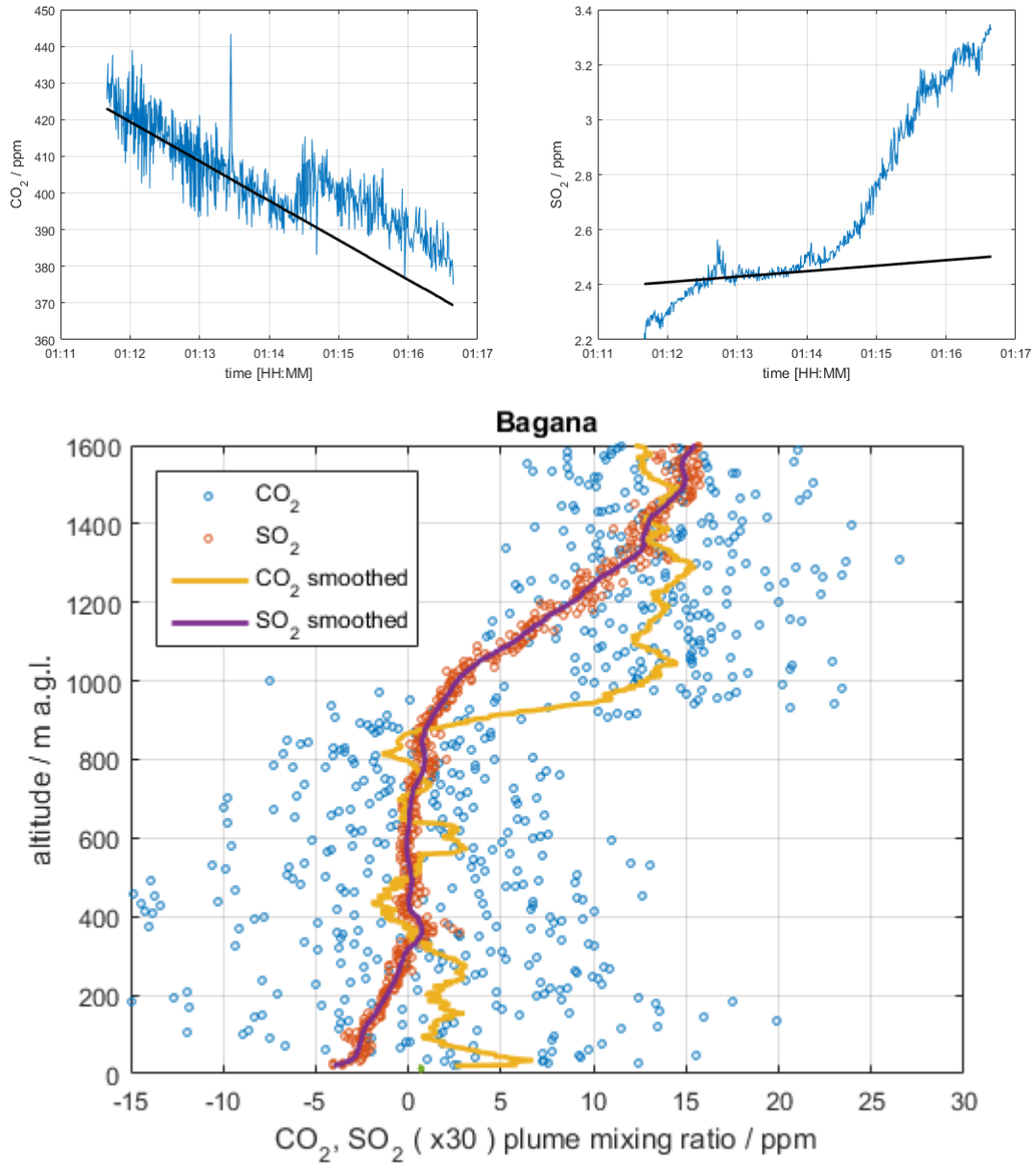
Figure 7. Method to derive the molar ratio in drone flights. The upper plots show the time-series obtained in Bagana of the mixing ratios for both species during ascent (blue), after calibration and time-response correction. Baselines are fitted in the region outside of the change of trend in the series, which are then extrapolated to the entire series (black). The molar ratio is then calculated by subtracting these background signals from the original signals. The data points and smoothed profiles are shown in the lower plot. The ratio CO_2/SO_2 is calculated from the areas of these curves around the regions of maximum mixing ratio

Figure 8. Calculation of the CO_2/SO_2 ratio for Ulawun. See Figure 7 caption for details

5. Results

The results of the measurement campaign are summarized in Table 3 below. We excluded the two fumarolic samples taken in the crater of Tavurvur, because they presented high hydrothermal contamination, evidence by low temperatures (33−36 °C) and high relative humidity (92−94%). We also excluded analysis for the second drone measurement at Bagana and the first in Ulawun, because they did not reach high plume concentrations or anomalous drifts (see raw data in Annex I). In general, it was also observed that the profiles during descent were not identical to the profiles during ascent. This could have been caused by instrumental drifts, plume meandering or strong disturbance of the air parcels due to the air-flow of the drone propellers.

Table 3. Results from the gas measurements on volcanoes of PNG. The ranges of CO_2/SO_2 indicate the span obtained if the estimate is done in the region of maximum concentration or in the entire plume. Red indicates the most probable value

Volcano	Measurement site	Period of valid measurement GMT	Particle filter	Teflon extension	Temperature °C	Pressure kPa	Relative humidity %	X_{H2O} %	X_{CO2}/X_{SO2} [ppm$_{mol}$/ppm$_{mol}$]
Tavurvur	Crater	2016-09-09 02:45-03:19	Y	Y	44.3 ± 2.9	98.87 ± 0.03	62.41 ± 8.12	5.54 ± 0.72	2.6
Bagana	Plume 1	2016-09-19 01:11-01:17	Y	N	32.4 ± 0.4	87.94 ± 5.14	55.99 ± 4.19	3.08 ± 0.11	$15.0 - 16.5$
Ulawun	Plume 2	2016-09-26 07:26-07:33	N	N	36.2 ± 0.2	85.67 ± 5.67	51.40 ± 8.07	3.60 ± 0.34	$4.8 - 7.3$

6. Discussion and conclusions

The most representative CO_2/SO_2 ratios were found to be 2.6 for Tavurvur, 15 for Bagana and 4.8 for Ulawun. These values were obtained in a region of ±20 data points around the regions of maximum mixing ratio of SO_2 (corresponding to a spatial extent of about $40-50$ m). Interestingly, the profiles of the two species are not identical, which would mean heterogeneities in the ratio within the plume. This has the effect of changing the ratio when the integration is performed in the entire profile, which has resulted in ratios of 16.5 or 7.3 for Bagana and Ulawun, respectively. We think however that the low mixing ratios in the border of the plume may be responsible for the apparent heterogeneity and regard the values obtained in the higher-concentrated parts more reliable.

It is unknown the extent to which carbon and sulfur is emitted or converted to other species, but it is expected that the C/S ratios are lower than the values stated before, as it is more likely that some sulfur is emitted as H_2S or emitted/converted to sulphate aerosol, or scrubbed by water droplets or ash.

The sources of uncertainty are several. On one hand, the precision of the instruments is supposed to be about 2%. On the other hand, the conversions of the raw signals into mixing ratios involve a series of steps (pressure compensation, calibration, time-response correction, background subtraction), which add some uncertainty to the result. Finally, there are dynamic processes during the measurement (plume meandering, water/ash contamination, variable background mixing ratios), which are manifested by a variance in the results. However, the results show relatively good precision in spite of all these changing conditions.

Future improvements of this concept include:

- Possibility to log the flight data (time, altitude, coordinates)
- Possibility to read the SO_2 signal in real-time as a marker of the location of the plume
- A common, and if possible, faster response time for the gas sensors
- A better exposure of the thermometer to ambient temperature
- Longer time of operation with better batteries

Given the limitation with the power, due to the impossibility to transport the best battery package, we have a serious constraint on the effective time of measurement. With longer autonomy, it would be possible to flight even higher, and more importantly, to sample inside the plume at a stationary position for longer time and then perform a measurement of the background mixing ratio at the same altitude.

This study demonstrates the applicability of a compact Sunkist system aboard a multi-rotor for measurements of volcanic gases at high elevations and challenging plume-atmospheric conditions.
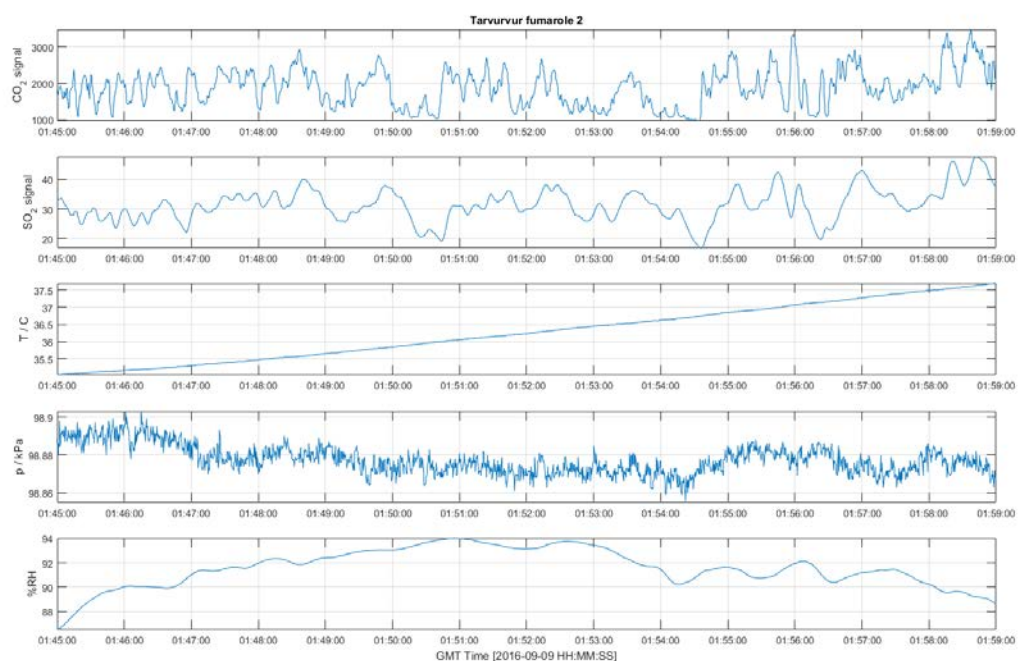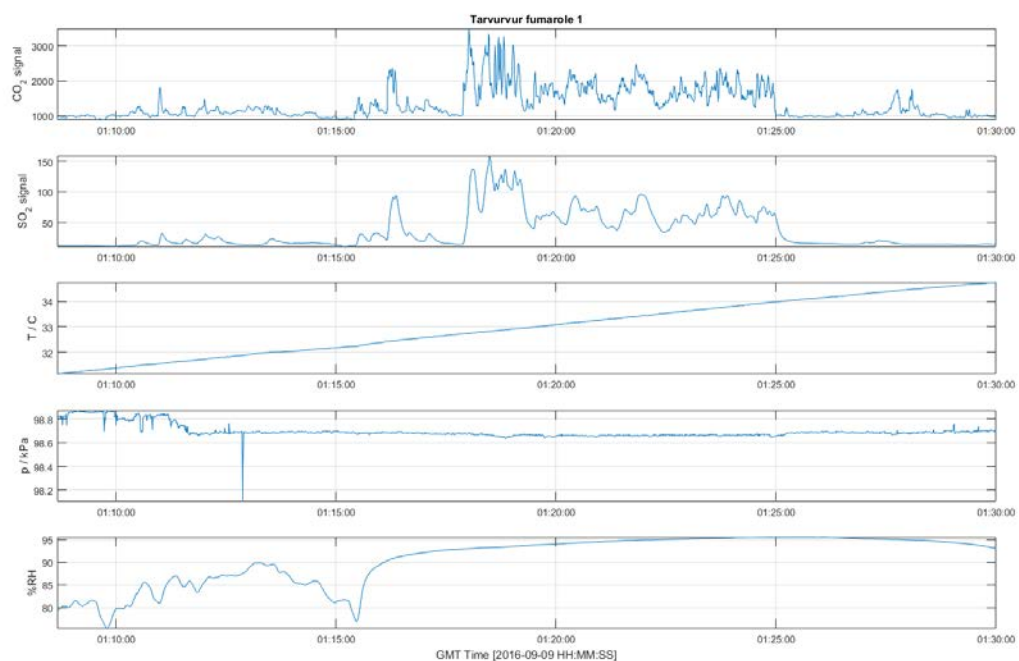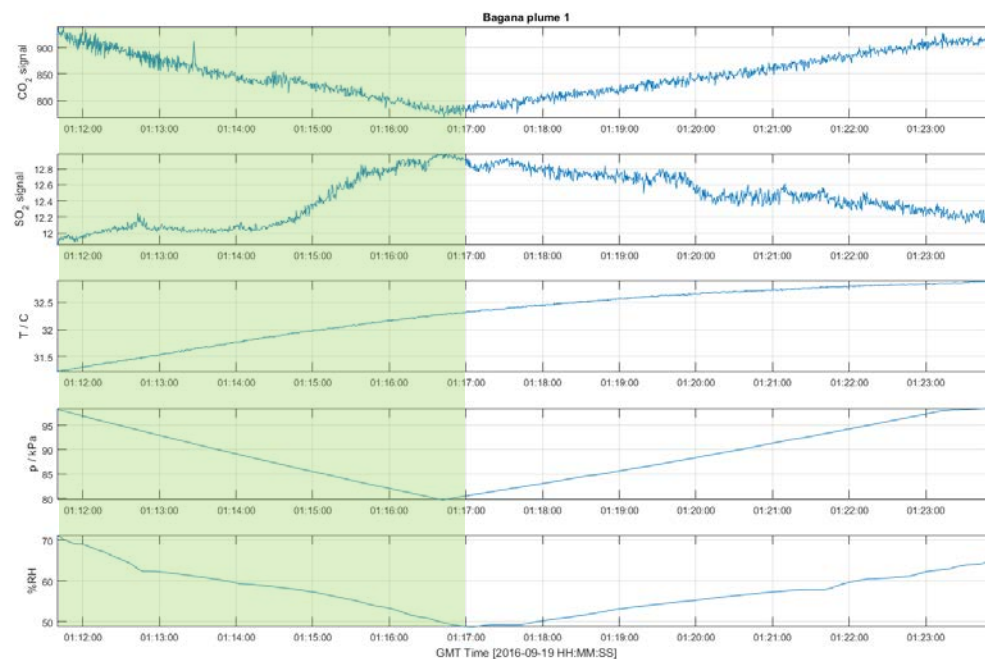
Acknowledgements

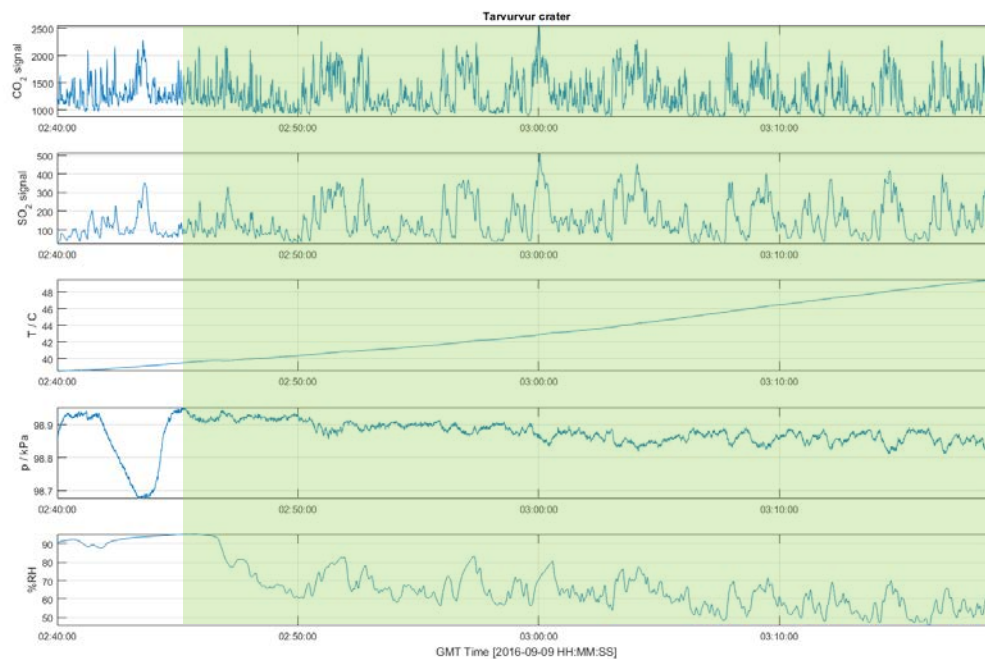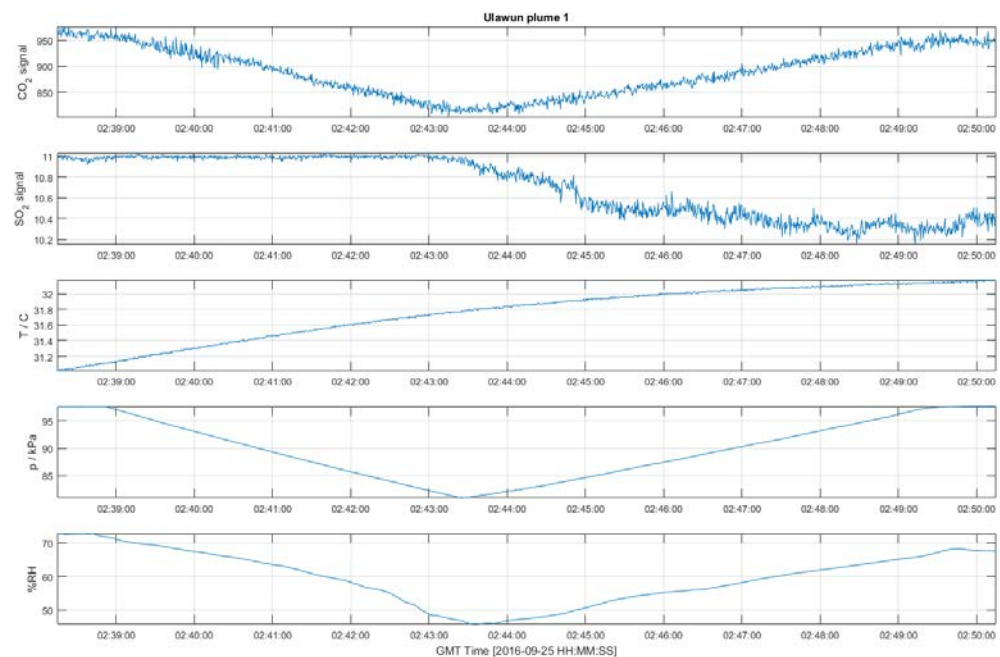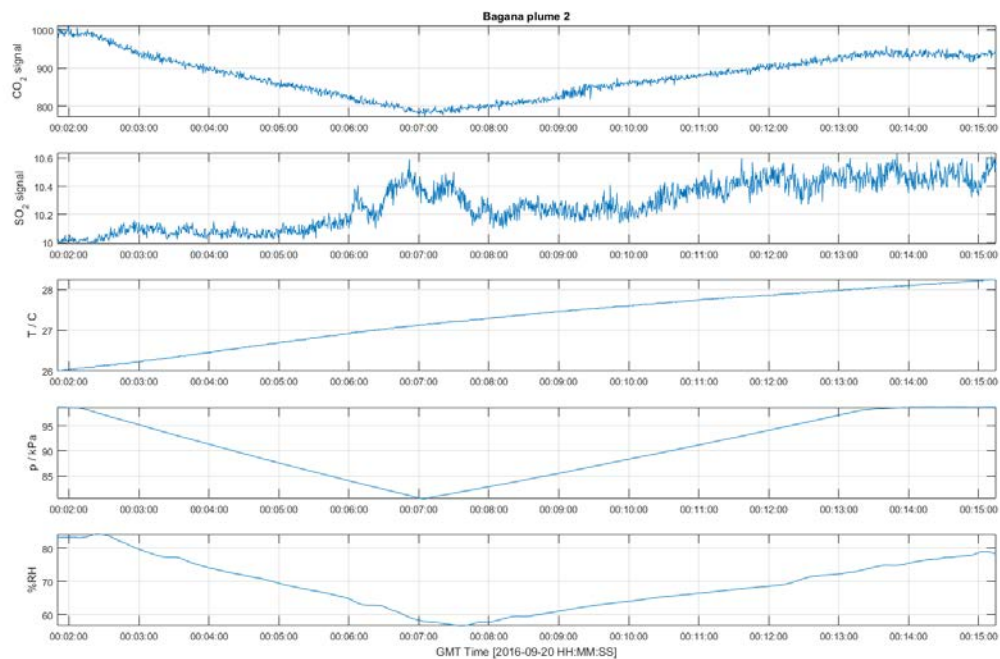## References

Amici S, Turci M, Giammanco S, Spampinao L, Giulietti F (2013) UAV thermal remote sensing of an Italian mud volcano. Adv Remote Sens 2:358–364.

Diaz J, Pieri D, Arkin C, Gore E, Griffin T, Fladeland M, Bland G, Soto C, Madrigal Y, Castillo D, Rojas E, Achí S (2010) Utilization of in situ airborne MS-based instrumentation for the study of gaseous emissions at active volcanoes. Intern J Mass Spectrom 295:3 105-112

Jensen M.E., Burman R.D., Allen R.G., (1990). Evapotranspiration and irrigation water requirements, ASCE Manuals and Reports on Engineering Practice No. 70. Am. Soc. Civil Eng., New York, NY. (332 pp).

Jordan BR (2015) A bird's eye view of geology: the use of micro drones/UAVs in geologic field work and education. GSA Today 25:50–52. doi:10.1130/GSATG232GW.1

Kaneko T, Koyama T, Yasuda A, Takeo M, Yanagisawa T, Kajiwara K, Honda Y (2011) Low-altitude remote sensing of volcanoes using an unmanned autonomous helicopter: an example of aeromagnetic observation at Izu-Oshima volcano, Japan. Int J Remote Sens 32:1491–1504.

Kelly PJ, Kern C, Roberts TJ, Lopez T, Werner C, Aiuppa A (2013) Rapid chemical evolution of tropospheric volcanic emissions from Redoubt Volcano, Alaska, based on observations of ozone and halogen-containing gases. J Volcanol Geotherm Res 259:317–333

McGonigle A. J. S., A. Aiuppa, G. Giudice, G. Tamburello, A. J. Hodson, and S. Gurrieri (2008), Unmanned aerial vehicle measurements of volcanic carbon dioxide fluxes, Geophys. Res. Lett., 35, L06303, doi:10.1029/2007GL032508.

Mori, T., Hashimoto, T., Terada, A., Yoshimoto, M., Kazahaya, R., Shinohara, H. & Tanaka, R. (2016). Volcanic plume measurements using a UAV for the 2014 Mt. Ontake eruption. Earth, planets and space 68, 49.

Shinohara H (2013) Composition of volcanic gases emitted during repeating Vulcanian eruption stage of Shinmoedake, Kirishima volcano, Japan. Earth Planets Space 65:667–675. doi:10.5047/eps.2012.11.001
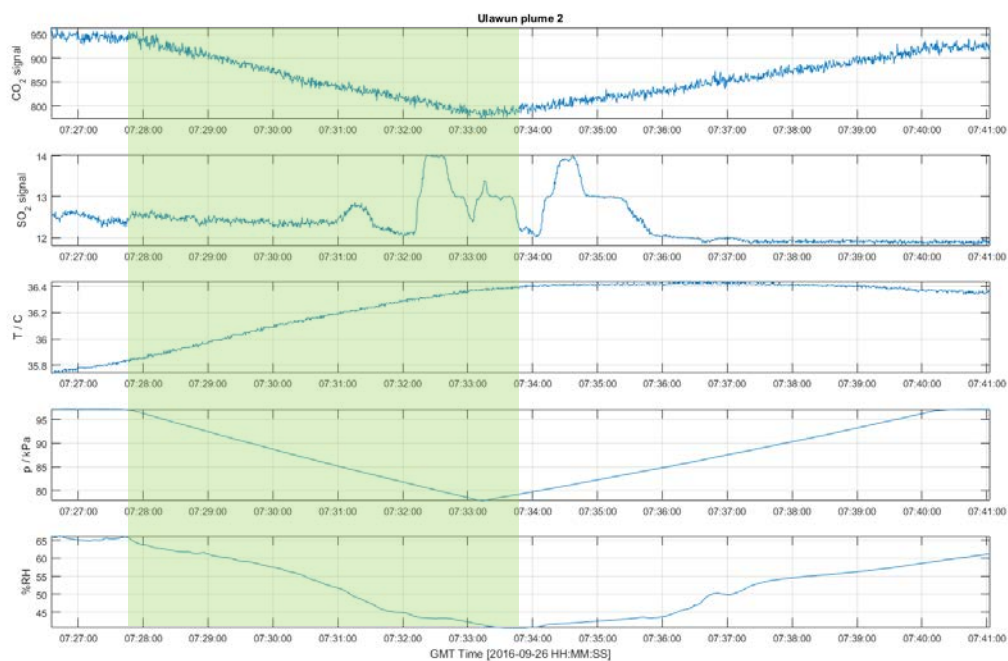
Annex

Plots of the raw data from the seven measurement sets taken at PNG

Tarvurvur fumarole 1

Tarvurvur fumarole 2

Tarvurvur crater

Bagana plume 1

Bagana plume 2

Ulawun plume 1

Figure A1. Raw data from the seven measurement sites at PNG. Shaded area indicates data windows used for analysis

New concept for gas monitoring of Tavurvur volcano, PNG

Wide field of view-dual beam scanning DOAS - Installation report

S. Arellano[a], B. Galle[a], J. Wallius[b], K. Mulina[c], I. Itikarai[c], J. Bosco[c], Ezequiel[c]

[a]Department of Earth and Space Sciences, Chalmers University of Technology, Gothenburg, Sweden

[b]Department of Earth Sciences, Uppsala University, Uppsala, Sweden

[c]Rabaul Volcano Observatory, Rabaul, Papua New Guinea

santiago.arellano@chalmers.se, bo.galle@chalmers.se

Introduction

Tavurvur volcano (-4.239, 155.21, 223 m) is one of the most well monitored volcanoes by the Rabaul Volcano Observatory (RVO) in Papua New Guinea (PNG). The flux of SO_2 is permanently monitored by a NOVAC-I scanning-DOAS system installed in the premises of Rabaul Hotel by the VDAP/RVO collaboration in 2015, as well as by frequent car-traverses with a FLYSPEC system, normally conducted from Rabaul (Fig. 1). Both methods are remote sensors which measure the amount of skylight UV radiation absorbed by the volcanic gas and derive the emission rate by the DOAS method and additional information of the gas transport speed and geometry of observation.

After the last eruptive activity in 2014, Tavurvur has maintained low levels of degassing, essentially fumarolic activity and weak passive degassing from a central vent. The gas usually accumulates inside the crater and is sporadically released to the atmosphere, producing puffs with little or null presence of ash. Both the stationary and mobile measurements are conducted at distances of >5 km from the volcano. The observation distance, and the low elevation and gas content of the emission makes the detection of SO_2 very challenging.
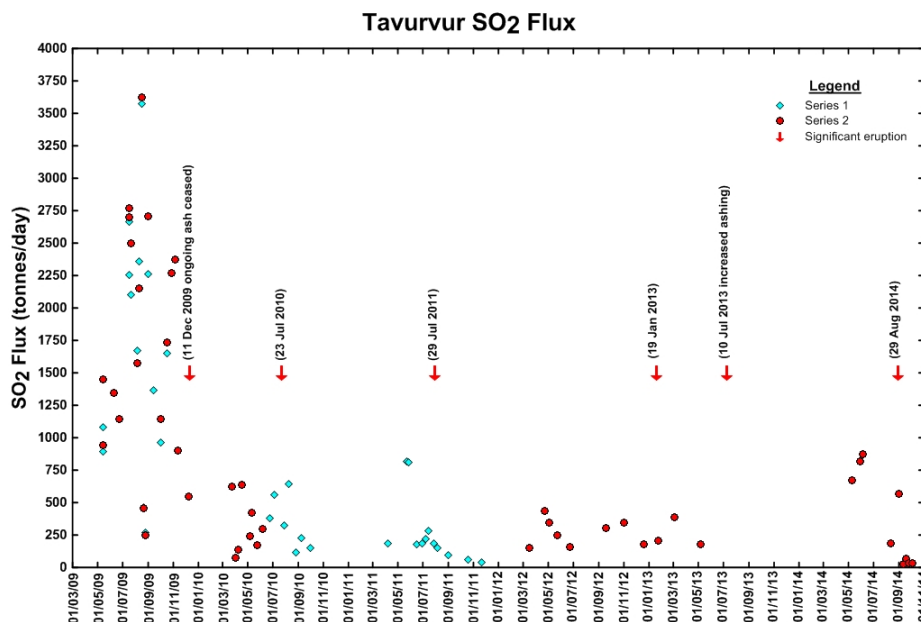
Figure 1. Time series of SO2 flux measurements at Tavurvur volcano produced by RVO (courtesy K. Mulina). The record was produced mostly from FLYSPEC traverses

During the September 2016 DECADE campaign in PNG, Chalmers conducted several stationary and mobile DOAS measurements around Tavurvur, evidencing the difficulty in obtaining gas flux records on this volcano by standard scans/transects from a point below the gas puffs. Consequently, an alternative concept for the measurements has been proposed, consisting in observing the emission at

a fixed position close to the point of emission. A similar approach has been adopted for early detection of eventual opening of closed volcanic systems, such as the case of Hekla volcano in Iceland. Ideally, the observed region of sky should be large enough to cover the entire cross-section of the plume, but not too large to include regions of gas-free sky that would dilute the derived gas column density. The use of a cylindrical lens allows transforming the circular field of view of a standard NOVAC scanner (8 mrad) into a rectangular field of view (8 mrad × 133 mrad). In this configuration the total amount of gas in a cross-section of the gas plume is integrated optically instead of by adding evaluated columns from a set of consecutive spectra in a traverse or scan. For high gas columns non-linearity effects complicates this "optical averaging". However, for low columns, as is the case here, the method is applicable. Moreover, by using the concept of dual-beam measurements, the observed sectors are duplicated and by simultaneously measuring two spatially separated regions of the plume, the transport speed can be calculated by cross-correlation of the shifted gas column density time series. In consequence, combining scanning DOAS with wide-field-of-view optics and a dual-beam spectrometer results in a very sensitive gas emission rate sensor which may be ideal for detecting gas under the present conditions at Tavurvur (Fig. 2).
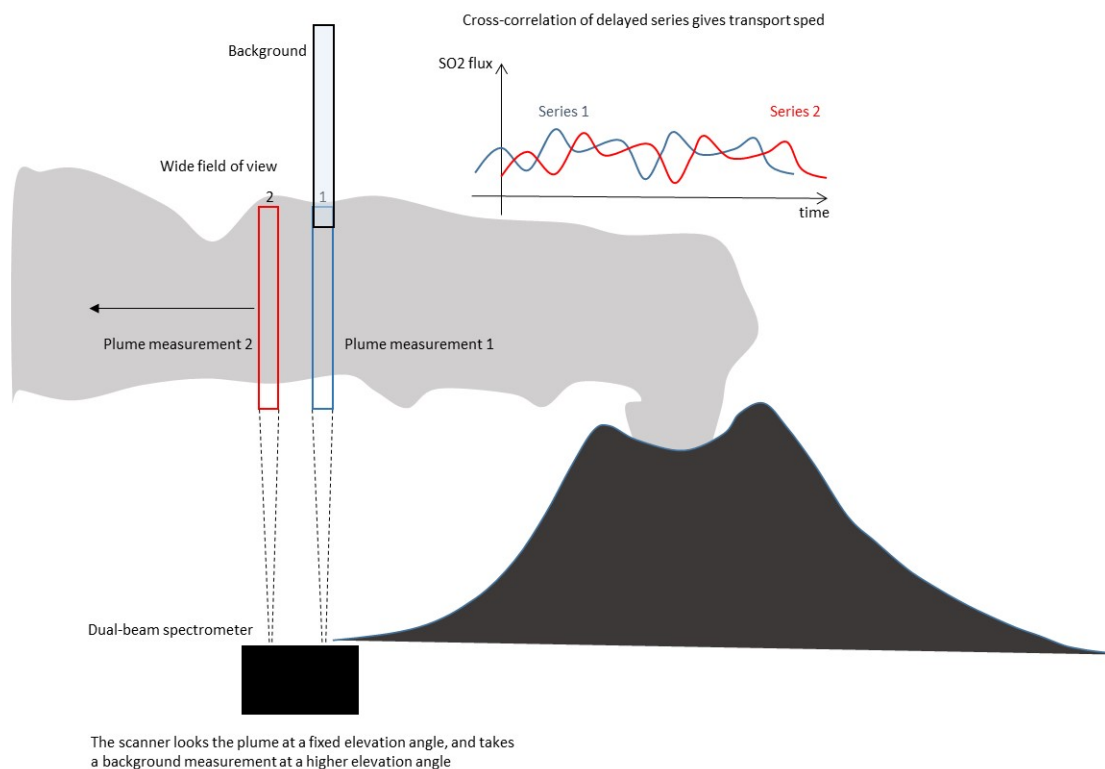
Figure 2. Sketch of the principle of measurement by a wide-field-of-view dual beam scanning-DOAS instrument

Installation site at Matupit

To obtain quantitative results of the gas emission rate ideally the sensor should observe the plume from a side. Since the predominant wind direction is southwesterly, a scanner could be looking from the north-west or south-east of the volcano. Furthermore, the observation geometry should be such that the weak gas plume can be observed against a gas-free sky background, i.e. no topographical obstacles should exist behind the plume. Considering these requirements, as well as for logistical and

security reasons, RVO suggested a site in the Matupit village, where an RVO monitoring/telemetry site is in place. After preliminary inspection of the site, it was concluded that the mast used for the transmission antennas offers a good viewpoint for the scanner.

A team composed of RVO and Chalmers scientists worked on the preparation and installation of the instrument between 28 September and 2 October 2016. The following stages were completed:

- General planning and discussion
- Building of platforms for the station
- Setting-up the components in a compact Peli-case
- Configuration and testing of the instrument
- Test of the telemetry
- Mounting of the instrument and telemetry
- Tests of azimuth and elevation angles of the scanner
- Final tests of the system and data transmission to RVO

It was noted during the installation the failure of two components of the system: a timer used to control the operation time of the instrument and the electronic distribution unit. These components were replaced, solving the problems, but it was informed by RVO that similar failures occur after the installation of the stationary system at Rabaul Hotel. Chalmers will explore the possible causes of these problems.

The coordinates and characteristics of the scanner are shown in Table 1, and Figure 3 shows the location and pictures of the station. The distance to the topographical obstacles in the viewing direction is 3.2 km, while the distance to a plume drifting towards north-west is about 2 km. This results in a typical separation between vertical observed sectors of 160 m and a width of the sectors of about 266 m.

Table 1. Coordinates and characteristics of the scanner

Name	Matupit
Latitude	− 4,243760
Longitude	152,190128
Altitude	32 m asl
Tilt angle	0 deg
Cone angle	90 deg
Spectrometer serial number	D2J2355
Compass direction	328 deg
MotosStepComp	119
IP address	192.168.1.33
Activation time of the timer	7:00 – 18:00 LT
Activation time of the program	8:00 – 17:00 LT
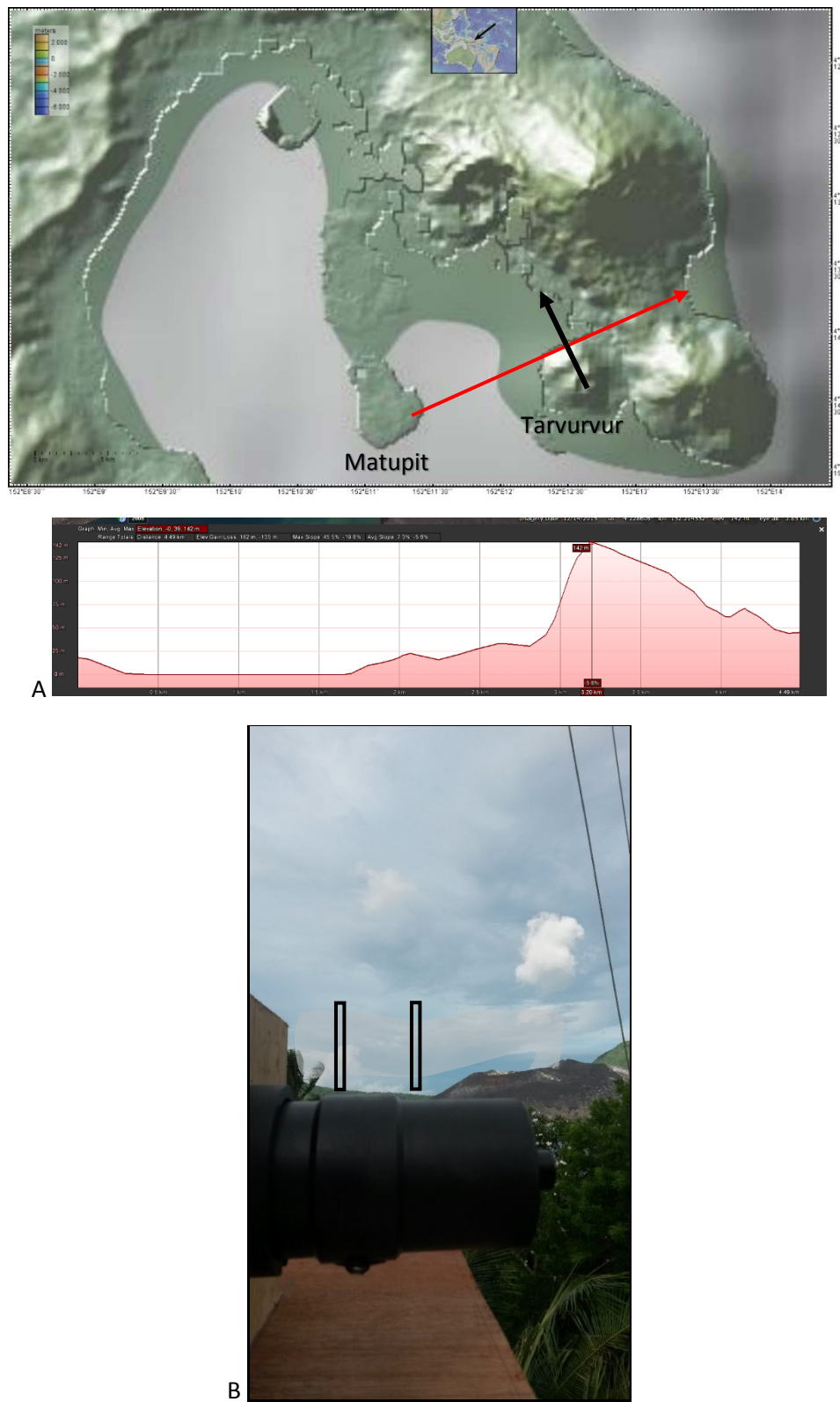
Figure 3a. (A) Location of the station, viewing direction (red), typical direction of the plume (black) and topographic profile in the viewing direction. (B) Photograph of the viewing direction with a sketch of an emission and approximate size of the viewed sectors of the plume at 2 km distance

Figure 3b. (C) Instrument in the lab. (D) Instrument installed in the mast of the RVO Matupit station, viewed from north. The scanner is mounted on a platform which also offers shadow to the Peli box containing the instruments. Data and power cables are connected to the existing radio/power installations inside the Japanese Bunker

Measurement modes

Two measurement strategies were tested during October 2016: 'sensitive detection' and 'average flux'.

Sensitive detection:

In this mode, one channel of the spectrometer measures at full spectral resolution and an averaging time matching the fluctuation rate of the emission (typically 30 s), allowing frequent and sensitive detection of the total column density of SO_2. In order to obtain fluxes in this mode, the wind speed needs to be obtained from external data.

Average flux including plume speed:

In this mode, the two channels of the spectrometer are used to simultaneously measure, with high time resolution (1 sec), in 2 intersections of the plume, horizontally displaced in the plume propagation direction. This sampling is performed at a lower spectral sampling. Measurements are conducted for a typical duration of 30 min, producing two time series of SO_2 column density shifted in time. This mode allows dual-beam estimates of the plume speed and thus the average flux during the time of observation can be obtained without provision of additional plume speed information.

It must be noted that large column densities can result from gas emissions transported towards the station because in such situation the optical path through the gas can be large. In this case, the estimate of the flux must be done with care, as the extent and speed of the plume would be difficult to determine. However, the wind patterns make this situation atypical.

First results

The following plots show first results from the sensitive detection measurement mode.
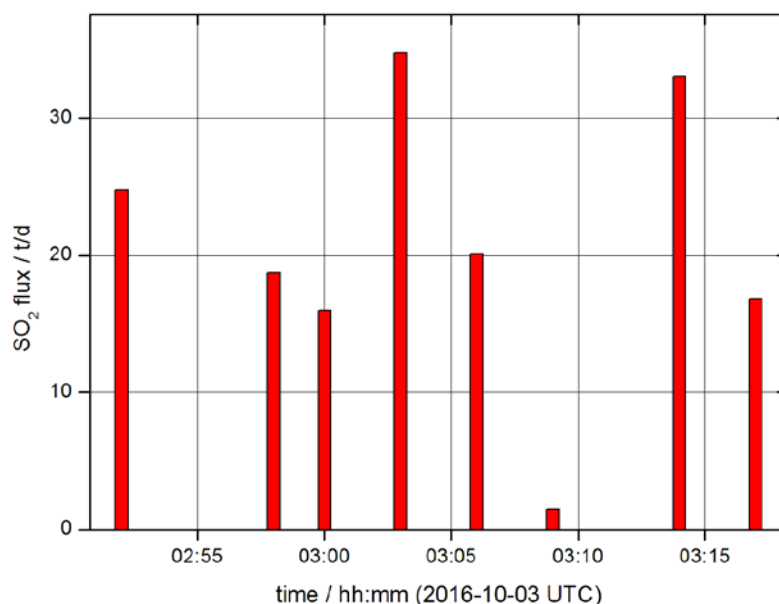
Figure 4. Time series of SO_2 flux measurements with the wide-field-of-view dual-beam scanning-DOAS system at Matupit in 'sensitive detection' mode. The plume speed is assumed to be 5 m/s in the direction normal to the viewing direction. The plume width is estimated at 333 m. The mean flux is 17 ± 4 t/d for the 3 October 2016

In the following figures is shown the results from 1 week of measurements in October 2017. During 2 days, 25 and 26 October, the "*average flux*" mode was used, to derive plume speed, Figure 5. An average plume speed of 3.9 ms^{-1} was obtained for the 2 days. This value of the plume speed was used in all the following flux evaluations.
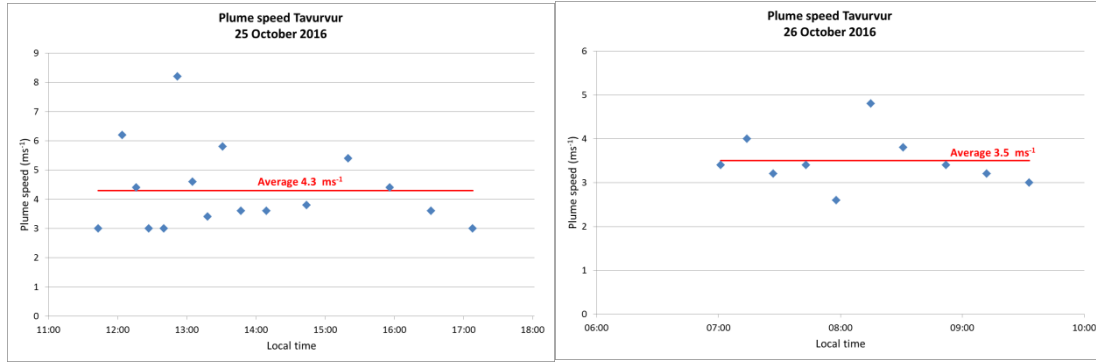
Figure 5. Plume speed measurements made downwind Tavurvur volcano 25 and 26 October 2017, using the WFOV-DOAS in "*average flux*" mode

In Figure 6 is shown a typical result from a measurement of the emission using the "*sensitive detection*" mode on 23 October. Plume speed used was 3.9 ms^{-1}.
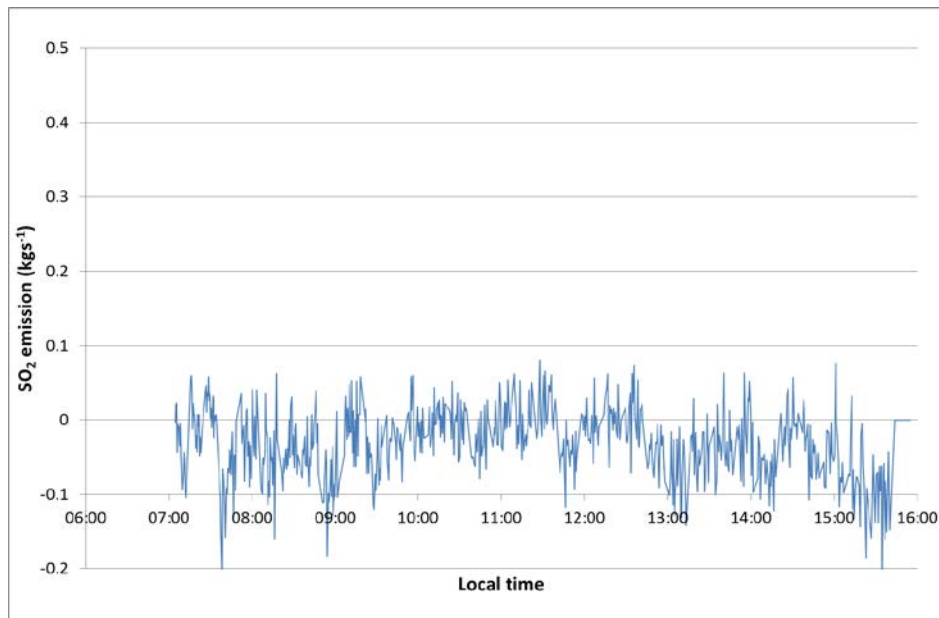
Figure 6. Measurement of the emission from Tavurvur volcano on 23 October 2017 using the WFOV-DOAS operating in *"sensitive mode"*

The measurement shown in Figure 6 consist of 34 individual measurement series, each comprising a clean air sky reference spectrum and 20 individual plume measurement spectra, each with a duration of 30-45 seconds. When evaluating the columns each one of the 20 plume spectra is divided by the preceding sky spectrum. Ideally the sky spectrum should be without SO_2. If the sky reference contains SO_2 then this will introduce an offset in the column value of the plume measurements. Unfortunately, in the case shown here there is varying amounts of SO_2 in the sky reference. This causes each of the 34 data-sets to have a different offset. These offsets can however be determined if one assumes that the last plume measurement in one data-set should have the same value as the first plume measurement in the following data-set. The difference in offset between the different data-sets can then be eliminated. This has been done in Figure 7. Here a systematic variation in the derived emission can be seen. This variation may be due to varying emission, or varying plume speed or plume direction. If no clean air reference is obtained during the day, then the figure only shows the relative emission. If however there is a clean air reference, caused for example by a changing wind direction, then the value of this sky reference can be used to fix the offset value. If one assumes that the lowest flux values

during the day represents little or no gas, then it is possible to use the span in the emission as an estimate of the real emission. It is however possible that this is an underestimation of the real emission.
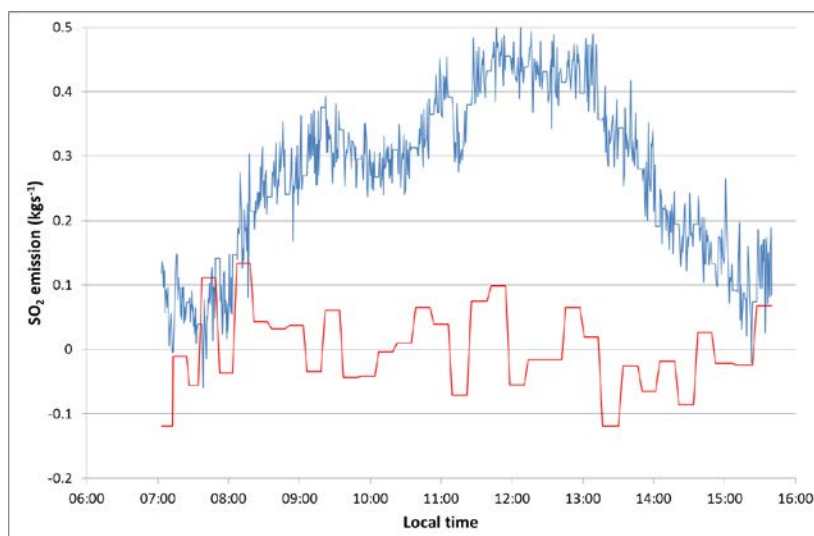
Figure 7. The emission measurements shown in Figure 6, after correction for different offset caused by varying amount of SO_2 in the clean air reference spectra. In red is shown the offset correction values

Examining the location of the clean air sky reference it can be seen that this is taken at an angle of only 13° above the horizon, as compared to the plume measurement that was taken 6° above the horizon. Given the large vertical FOV of the instrument this means that the clean air sky spectrum is likely to contain SO_2 from the plume. In the future, lifting the sky reference 5-10° should eliminate this problem, and provide a clean and stable clean air reference.

In Figure 8 is shown the average emission during one week in October 2017, derived using the above described methodology.
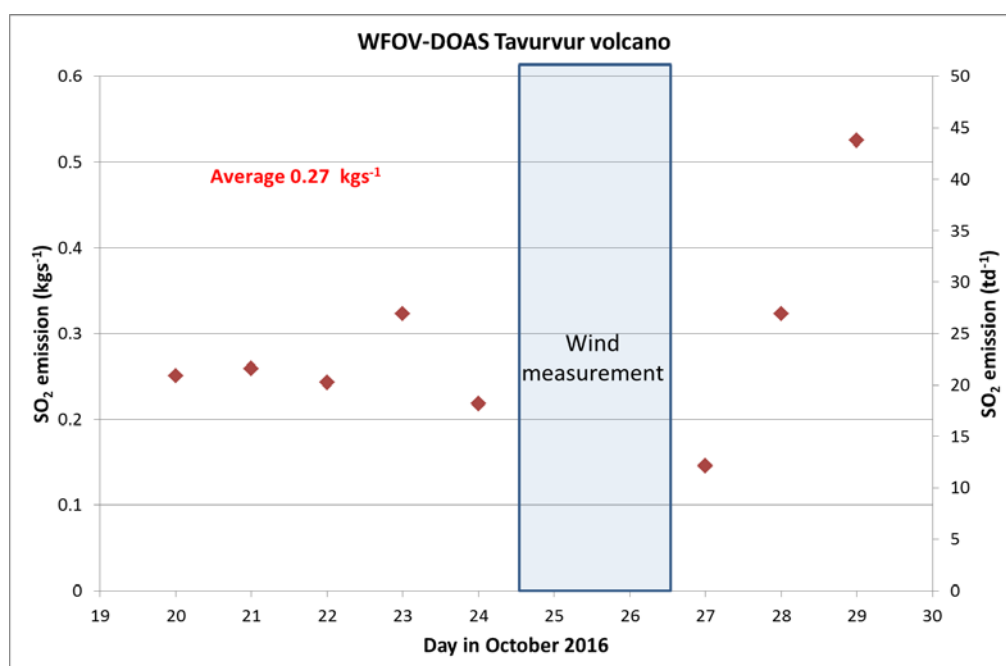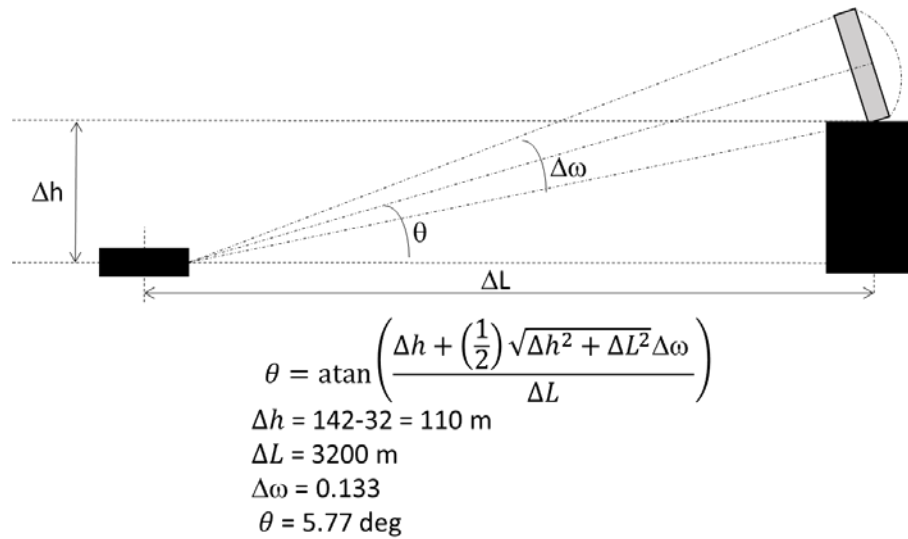

Figure 8. Average SO_2 emission from Tavurvur volcano derived from measurements with the WFOV-DOAS located at Matupit Island

8

Determination of elevation angle

It is important to determine the correct elevation angle of the scanner to ensure observing the plume against a clear sky background. Too low elevation angles could result in the scanner hitting a mountain or other obstacle and thus not obtaining enough UV radiation from behind the plume. Too high elevation angles could result in the scanner looking the clear sky, especially since the emission is weak and not elevated.

The elevation angle for the station at Matupit was optimized in the field by looking at the intensity of radiation in the two spectrometer channels at different angles, both in elevation and azimuth. With help of a map, these angles were checked and a calculation of the optimal angle is based on the sketch shown in Figure 9.

$$\theta = \mathrm{atan}\left(\frac{\Delta h + \left(\frac{1}{2}\right)\sqrt{\Delta h^2 + \Delta L^2}\,\Delta\omega}{\Delta L}\right)$$

Δh = 142-32 = 110 m
ΔL = 3200 m
$\Delta\omega$ = 0.133
θ = 5.77 deg

Figure 9. Estimation of the elevation angle of the scanner. The box on the left represents the position of the scanner and the box on the right, the position of the highest obstacle in the viewing direction of the telescope. The telescope has a characteristic field of view (133 mrad in the vertical). From this information an elevation above the horizontal of 5.77 deg is derived, which would correspond to 3-4 steps of 1.8 deg of the stepper motor of the scanner

Configuration files of the measurement modes

In this annex, the general and specific parameters of the configuration file of the instrument are detailed for the two modes of measurement.

General parameters

```
STARTCHN=0                  % Initial active channel of the spectrometer
STOPCHN=2047                % Final active channel of the spectrometer (full spectrum)
REALTIME=0                  % Used to move the scanner
STEPSPERROUND=200           % Number of steps of the stepper motor to complete a revolution
MOTORSTEPSCOMP=119          % Number of steps of the stepper motor to find the zenith position
SKIPMOTOR=0                 % Use to move the scanner
DELAY=200                   % Time in ms between steps of the scanner
POWERSAVE=0                 % Used to move the scanner
PERCENT=0.9                 % Factor of scale of the maximum intensity of the spectrum (1 means saturation)
MAXINTTIME=1000             % Maximum time in ms for the exposure time of the spectrometer
DEBUG=1                     % Used to log information
CONEANGLE=90                % Shape angle of the scanner (90 for flat, 60 for conical)
COMPASS=328.0 0.0 0.0       % Only the first number is defined for the azimuth of the scanner
```

Parameters specific for 'sensitive detection'

```
%-----pos----time-sum1-sum2--chn--basename----- repetitions-----flag
MEAS=43 -1 15 5 0 sky 1 0              % Position and acquisition parameters for the sky spectrum
MEAS=100 0 15 5 0 dark 1 0            % Position and acquisition parameters for the dark spectrum
MEAS=47 0 15 5 0 scan 20 0            % Position and acquisition parameters for the plume spectra
```

Parameters specific for 'average flux'

```
%-----pos----time-sum1-sum2--chn--basename----- repetitions-----flag
MEAS=43 -1 5 1 257 sky 1 0            % Position and acquisition parameters for the sky spectrum
MEAS=100 0 5 1 257 dark 1 0          % Position and acquisition parameters for the dark spectrum
MEAS=47 0 5 1 257 wind 400 0        % Position and acquisition parameters for the plume spectra
```